# On the Design Details of SS/PBCH, Signal Generation and PRACH in 5G-NR

## ARVIND CHAKRAPANI<sup>ID</sup>, (Member, IEEE)
Qualcomm Technologies, Inc., Bridgewater, NJ 08807, USA
e-mail: achakrap@qti.qualcomm.com

**ABSTRACT** The 3rd Generation Partnership Project (3GPP) specification of the fifth generation (5G) New Radio (NR) allows for a highly scalable and flexible radio access technology to cater to network operators with different requirements. Such scalability and flexibilities in network configurations inevitably translate to complications in the design and implementation of 5G-NR systems. Radio access in 5G-NR is much more complex and involved than its predecessor, 4G long term evolution (LTE) and LTE-Advanced technology. Therefore, the 5G-NR specifications turn out to be quite dense. Specifically, the specifications are concise, design motivations rarely explained, and the information can be convoluted or distributed across several documents. Moreover, there are several key design details associated with the access layer procedures for any given physical layer channel, which are often omitted in the specifications. For example, design motivation aspects of initial access channels or signal generation can be quite difficult to follow or understand in 5G-NR. In this paper, all the design details associated with initial access channels and signal generation in 5G-NR specifications are laid out. The contributions of the paper are three folds. First, the design details and justifications associated with both downlink and uplink access channels are presented along with signal generation details. Secondly, receiver design aspects of NR PRACH short formats are discussed. Lastly, PRACH receiver implementation aspects and performance reports from different network operators are presented and compared with 3GPP specified Radio Performance and Protocol aspect requirements for millimeter wave (mmW) access. The work in this paper is of significant value to researchers and system engineers looking to design and build initial access algorithms as part of 5G NR systems.

**INDEX TERMS** 3GPP, 5G-NR, 4G, LTE, OFDM.

## I. INTRODUCTION

With innumerous and radically diverse deployment scenarios in 5G-NR, the NR cell architecture should offer scalability and flexibility across an extreme variation in connectivity requirements [1]. Very high throughput (1 Gbps or more), ultra-low latency (order of 0.5ms in some cases), ultra-high reliability and mobility with low energy consumption are the key driving factors of 5G-NR. Towards this end, all the physical layers channels can be configured flexibly to cater for different scenarios. Such flexibility has led to a dense and complex specifications for physical layer procedures in 5G-NR. For example, for initial downlink access, the synchronization block (SS/PBCH) can be transmitted with a sub-carrier spacing (SCS) different than the carrier SCS for faster synchronization; different time placement pattern of SS/PBCH can be adopted (only for 30kHz SCS) to

accommodate NR-LTE coexistence; different patterns can be configured for the time/frequency placement of SS/PBCH and remaining system information (RMSI) blocks and so on. Further, SS/PBCH can be placed on a different sync raster than the regular channel raster (only option in LTE), for faster downlink synchronization by making synchronization blocks sparser in frequency (i.e., SS/PBCH placement at only given frequency locations). This facility requires calculations on the sync raster entries based on bandwidth configuration, SS/PBCH resource size, etc. For uplink initial access/synchronization, the random access (PRACH) channel supports several long and short formats for different coverages and combinations of formats (short) with configurable time/frequency placements. A PRACH preamble can have varying number of sequence repetitions depending on the format to provide different coverage range. There could also be several preambles within a slot to cater for multiple random access occasions. Support of formats with large repetitions or multiple PRACH occasions within a slot, increases the

The associate editor coordinating the review of this manuscript and approving it for publication was Larbi Boubchir<sup>ID</sup>.

receiver processing load at a 5G next generation-base-station (gNB) and therefore the gNB feature support capabilities should be carefully determined. Further, to help towards beam correspondence, different SS/PBCH to PRACH mapping are defined so that single/multiple SS/PBCH map to multiple/single PRACH occasions along with the regular one-to-one mapping. These mapping options have implications on the SS/PBCH and PRACH receiver processing complexity at the gNB. Also, if a common digital front end (DFE) chain is to be used for data and random access reception in the same slot, the PRACH receiver at gNB will be required to perform additional phase corrections due to cyclic prefix (CP) removal on the data channel.

As 5G-NR specification allows for different SCS which can be configured for initial access and data channels; provides flexibility of placing the resources on separate bandwidth parts (BWPs[1]), and therefore there are several frequency offsets parameters defined in the 3GPP physical layer procedures specification with complicated equations. These offsets are necessary for correct placements of resources and for correct OFDM signal generation and reception in 5G-NR. To understand all the details on design goals and motivations for SS/PBCH, PRACH channels and OFDM signal generation in 5G-NR, one must go through several 3GPP specifications and contributions. This could prove be a very difficult task for anyone not familiar with 3GPP standardization process and documentation. Moreover, information is scattered across a vast number of documents with nested references, making the task of connecting the dots a very tedious process.

The objective of this paper is to unwind all the design details associated with the initial access channels and illustrate them with examples wherever possible to help understanding better the overall design. Specifically, the following contributions are made in this paper. First, all the design details associated with downlink access channels and OFDM signal generation in 5G-NR are presented with examples. Secondly, design details of PRACH channel along with important receiver design aspects are presented. Finally, PRACH receiver implementation aspects and performance from different network operators are presented and compared with RAN4[2] recommended minimum requirements for millimeter wave (mmW) access. Rest of the document is organized as follows. In section 2, SSS/PBCH channel design details are provided with illustrations and examples. Section 3, details of the OFDM signal generation and phase pre-compensation at the transmitter are presented. Section 4 focuses on all the PRACH channel design aspects and details. Lastly, important aspects of the PRACH receiver design along with RAN4 performance from different network operators is presented and discussed.

---

[1]In 5G-NR, gNB can fragment the carrier bandwidth into smaller BWPs with similar or different subcarrier spacing [4]. This flexibility allows users with different bandwidth and device capabilities to operate within a smaller bandwidth part (BWP) compared to the carrier bandwidth.
[2]Radio Performance and Protocol aspect requirements are specified by the 3GPP Radio Access Network working group 4, also known as RAN4
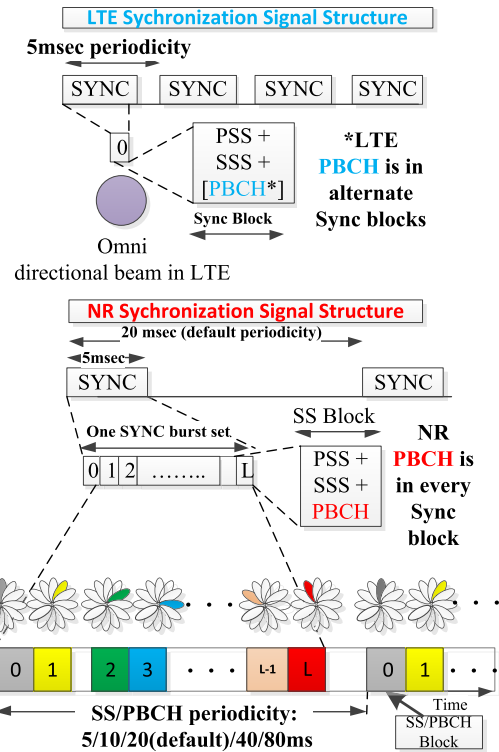
**FIGURE 1.** Synchronization signal structure in 4G-LTE and 5GNR.

## II. SS/PBCH DESIGN

SS/PBCH block transmission allows UEs to synchronize or lock to a cell. In NR, synchronization signal blocks constitute of a primary synchronization signal (PSS), a secondary synchronization signal (SSS), and a physical broadcast channel (PBCH). Unlike LTE, which has PSS/SSS transmitted every 5ms and PBCH transmitted every 10ms, the three SS/PBCH components in NR are always transmitted together (i.e., they all have the same periodicity). As illustrated in Figure 1, a given SS/PBCH is repeated within a set of SS/PBCH transmissions, which can be used for gNB beam-sweeping transmission [2]. One or multiple SS/PBCHs compose an SS/PBCH set as indicated in Fig 1. The SS/PBCH set is confined to a 5 ms window and transmitted periodically. For initial cell selection, the user equipment (UE) assumes a default SS/PBCH set periodicity of 20 ms, but subsequently this periodicity can be configured to be 5/10/40/80/160 ms depending on need to make SS/PBCH more frequent or sparser. Synchronization during initial access is a two-step identification process (via PSS and SSS) to provide for both timing (only symbol and slot) and frequency synchronization. PBCH demodulation will reveal system frame number and enable reception of control/data channels (PDCCH/PDSCH). Detection of RMSI (transmitted over regular PDCCH/PDSCH) may be necessary during initial access for UE to perform random access (via PRACH). However, transmission of RMSI itself is optional to gNB (for non-standalone or NSA mode) and the presence or absence of RMSI is indicated in the PBCH block. Note that SS/PBCH transmission can also be

used for signal measurement purposes at the user equipment (UE) and only those SS/PBCH associated with an RMSI are referred to as a Cell-Defining SS Block (CD-SSB) (see section 5.2.4 of [4]). PSS/SSS/PBCH can be transmitted with SCS of 15/30kHz for frequency range 1 (i.e., FR1 or sub-6 bands) and with SCS of 120/240kHz for frequency range 2 (i.e., FR2 or mmW bands). However, RMSI is defined only for SCS of 15/30kHz for FR1 and SCS of 60/120kHz for FR2 [2]. This is mainly to cater for different channel conditions and different coverages with different frequency ranges. The SS/PBCH set contents, including the maximum number of SS/PBCHs within an SS/PBCH set, SS/PBCH mapping pattern, and SS/PBCH set mapping to slots in a radio frame is also carrier-frequency-dependent.

Regardless of the SS/PBCH set composition, the transmission of SS/PBCHs within an SS/PBCH set is confined to a 5 ms window. The maximum number of SS/PBCHs within an SS/PBCH set (i.e., within 5ms period) is specified to be 4 for frequency ranges up to 3 GHz, 8 for 3 to 6 GHz, or 64 for 6 to 52.6 GHz in order to achieve a trade-off between coverage and resource overhead. Furthermore, the number of actual transmitted SS/PBCHs is configurable and could be less than the maximum number. This option is particularly useful towards reducing processing burden at the gNB, especially in the case of requiring transmission of multiple SS/PBCHs on multiple carriers within a slot.

Within a broadcast channel (BCH) transmission time interval (TTI) period of 80 ms, there are 16 possible positions of an SS/ PBCH set if we consider the minimum period for an SS/PBCH set is 5 ms. The 16 possible positions of an SS/PBCH set could be identified by the 3 least significant bits (LSB) of the System Frame Number (SFN) and 1-bit half radio frame number index. The SS/PBCHs are repeated within an SS/PBCH set and when the UE detects an SS/PBCH, it can acquire the timing information from its PBCH, from which the UE can identify the radio frame number, the slot index in a radio frame, and the orthogonal frequency-division multiplexing (OFDM) symbol index in a slot. The timing information contains additional 6 bits for SFN, 1 bit for half radio frame index, and 2, 3, or 6 bits for SS/PBCH time index for frequency ranges up to 3 GHz, 3 to 6 GHz, and greater than 6 GHz, respectively. Within the SS/PBCH indices, two or three LSBs are carried by changing the demodulation reference signal (DMRS) sequence of PBCH. Thus, for the frequency ranges below 6 GHz, the UE can acquire the SS/PBCH index without decoding the PBCH. It also facilitates PBCH soft combining over multiple SS/PBCHs as these SS/PBCHs with different indices carry the same content of PBCH payload. SS/PBCH can be placed (in frequency) on channel raster (as in LTE) or the newly defined sync channel raster in 5G-NR.

## A. SYNC CHANNEL RASTER
Synchronization (or sync) channel raster identifies the set of possible frequency locations of the SS/PBCH, consisting the synchronization channels PSS/SSS and the PBCH. Unlike
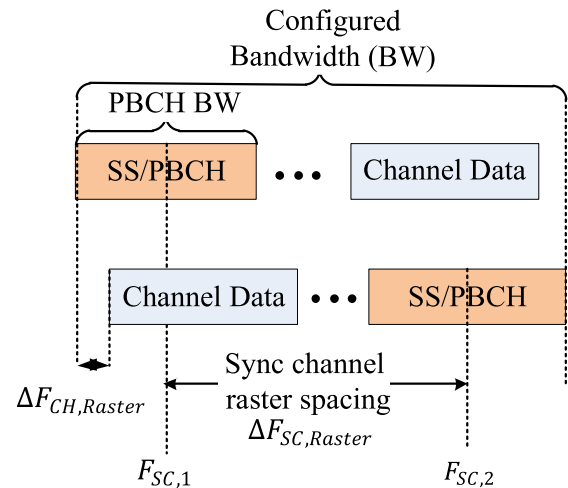


**FIGURE 2.** Sync and channel raster.

LTE, the SS/PBCH block in NR need not be in a fixed position within the configured bandwidth of the RF carrier but can be placed anywhere on the RF carrier bandwidth. This enables a sync channel raster that is sparser than the RF channel raster [5]. The advantage of having a sparser sync channel raster is a reduced search time for the initial access (less hypothesis to work with at the UE receiver). It relies on the SS/PBCH block bandwidth (i.e., PBCH bandwidth) being smaller than full channel bandwidth of the RF carrier transmitted from the gNB and that it is not in a fixed position within the configured bandwidth. The PBCH bandwidth of 240 subcarriers corresponding to 20 resource blocks (RBs) defines the flexibility of placing the sync channel. A primary cell (PCell) is always associated to a CD-SSB located on the synchronization raster. Note that in 5G-NR the definition of a physical resource block (PRB) is the same as LTE with 12 subcarriers constituting an RB, but the bandwidth of a PRB varies with the numerology or SCS being used.

The relation between the RF channel raster and sync channel raster is demonstrated with an example in Figure 2. In the example, two carrier positions 1 and 2 are shown leading to two different placements of the PBCH. The PBCH (and the SS) can be placed on a raster that is sparser than the RF carrier raster and those sync channel raster positions are denoted by $F_{SC,i}$. Position 1 is the highest (rightmost) position of the configured bandwidth on the RF channel raster where the PBCH can be related to the sync channel position $F_{SC,1}$, thus the PBCH occurs as far left as possible on the carrier. Position 2 is the next position on the RF channel raster, thus offset by $\Delta F_{CH,Raster} + \Delta F_{SC,Raster}$ from Position 1. The sync channel raster spacing $\Delta F_{SC,Raster}$ will be limited by the following equation:

$$\Delta F_{SC,Raster} \leq BW_{Config} - BW_{PBCH} + F_{CH,Raster}$$

where $BW_{Config}$ is the configured transmission bandwidth, $BW_{PBCH}$ is the PBCH and $\Delta F_{CH,Raster}$ is the channel raster spacing.
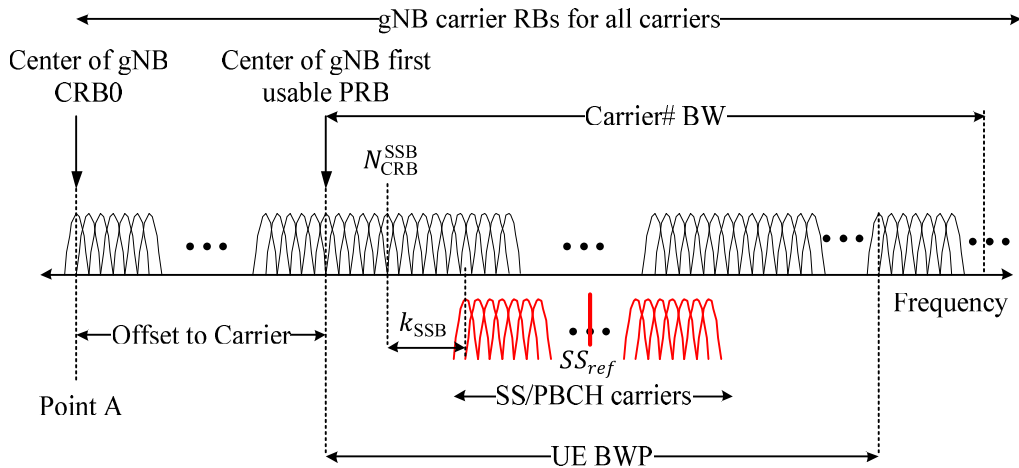
**FIGURE 3.** Alignment between SS block and channel RBs (see section 4.3.14 of [5]).

Sync raster is defined such that there is a minimum number of entries for each band [5] and raster entries are defined for each band (see section 4.3.1 of [5]). Sync raster entries will be defined for initial system acquisition, but SS/PBCH blocks can be transmitted by gNB in other frequency locations if the position is signaled to the UE explicitly[3] using the parameter $k_{\text{SSB}}$, which is derived from the frequency difference between the SS/PBCH block and Common Resource Block (CRB), also referred to as Point A in [3] ( see section 7.4.3.1 of [3] and section 13 of [7]). The SS/PBCH block is not RB aligned with the data RBs in the channel as shown in Figure 3. Instead, there is an arbitrary offset between the edge of the SS/PBCH block RBs and the edge of the data RBs in the channel and this offset can be up to 11 Resource Elements (REs) for mmW. Such placement enables multiple radio channels (with different NR-Absolute radio-frequency channel numbers or NR-ARFCN) that are subcarrier grid aligned but not RB grid aligned to use the same SS/PBCH block location. Hence, radio channels with different NR-ARFCNs that are offset by up to 11 REs in frequency can re-use the same SS/PBCH block frequency location.

The gNB places the SS/PBCH block at $SS_{ref}$ (one of the synchronization raster's). This is indicated by the red-line at the center of SS/PBCH block in Figure 3. The gNB also signals the offset (in number of subcarriers) between SS/PBCH block and the channel data RBs to help determine the control resource set for Type0-PDCCH common. This serves as an indirection for RMSI. Following parameters are signaled in RMSI for each supported SCS (each SCS is usually a different component carrier).

1. Absolute frequency of Point A - *absoluteFrequencyPointA* in *FrequencyInfoDL*, signaled as ARFCN NR

2. Offset in PRB units from Point A to the first usable PRB - *offsetToCarrier* in *SCS-SpecificCarrier*
3. Carrier bandwidth in PRB units - *carrierBandwidth in SCS-SpecificCarrier*
4. Sub-carrier spacing to determine the size of PRB - *subcarrierSpacing in SCS-SpecificCarrier*

Note that point A is RE#0 of RB#0 used to generate sequences for reference signals and scrambling. From section 7.4.3.1 of [3], the quantity $k_{ssb}$ is the subcarrier offset from subcarrier 0 in common resource block $N_{CRB}^{SSB}$ to subcarrier 0 of the SS/PBCH block, where the 4 least significant bits of $k_{ssb}$ are given by the higher-layer parameter *ssb-SubcarrierOffset* and for SS/PBCH block type A the most significant bit of $k_{ssb}$ is given by $a_{\bar{A}+5}$ in the PBCH payload as defined in subclause 7.1.1 of [3] (also see section 4, TS 38.212). The value $k_{ssb} \in \{0, \cdots, 11\}$ for FR2 and $k_{ssb} \in \{0, \cdots, 23\}$ for FR1. For FR2, or when $\mu \in \{2, 3\}$, the quantities $k_{\text{SSB}}$, and $N_{CRB}^{\text{SSB}}$ are expressed in units of resource blocks assuming 60 kHz subcarrier spacing. For FR1, or when $\mu \in \{0, 1\}$, the quantities $k_{\text{SSB}}$, and $N_{CRB}^{\text{SSB}}$ are expressed in units of resource blocks assuming 15 kHz subcarrier spacing (see section 4.2.2.2 of [3]). Figure 4 shows the computation of subcarrier offset $k_{ssb}$ for different numerologies of SS/PBCH and RMSI in FR1 and why $k_{ssb} \in \{0, \cdots, 23\}$ for FR1. The parameter $k_{ssb} \in \{0, \cdots, 11\}$ for FR2, since SS/PBCH is defined only for 120/240kHz and RMSI is defined only for 60/120kHz and that the configuration of SS/PBCH at 60kHz and RMSI at 120kHz is not valid (and hence 12 values for $k_{ssb}$ suffice).

**B. CRB TO SS/PBCH OFFSET EXAMPLES**

The common resource block and sub-carrier offsets to SS/PBCH should be computed in terms of subcarrier spacing of SS/PBCH for correct placement of the resources in frequency. In [3] however, for FR2, or when $\mu \in \{2, 3\}$, the quantities $k_{\text{SSB}}$, and $N_{CRB}^{\text{SSB}}$ are expressed in units of

---

[3]This is handled by gNB by setting the Master Information Block (MIB) parameter *ssb-SubcarrierOffset*(or the PHY parameter $k_{\text{SSB}}$) as $k_{\text{SSB}} > 11$ for FR2 or $k_{\text{SSB}} > 23$ for FR1 (see section 4.1 of [7]).
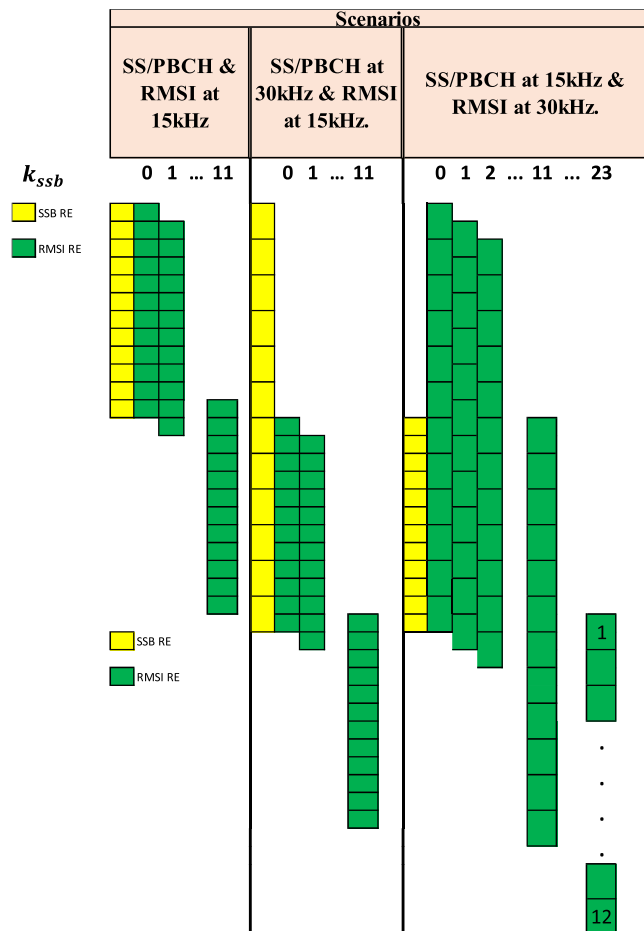
**FIGURE 4.** Subcarrier offset $k_ssb$ in FR1.

resource blocks assuming 60 kHz subcarrier spacing. Let, $SSB_{CRB}^{offset}$ represent the offset from point A to the closest common resource block before SS/PBCH. Let, $SSB_{sc}^{offset}$ be the subcarrier offset from subcarrier 0 in common resource block $SSB_{CRB}^{offset}$ to subcarrier 0 of the SS/PBCH block assuming sub-carrier spacing of SS/PBCH. The SSB CRB offset ($SSB_{CRB}^{offset}$) and subcarrier offset ($SSB_{sc}^{offset}$) are illustrated for FR2 in Figure 5. For FR2, SS/PBCH can only use either 120kHz or 240kHz subcarrier spacing. The first tone of SS/PBCH block (or the PBCH tone) can only begin at the center (or peak) of a 120kHz/204kHz subcarrier. This means that $k_{ssb} \in \{0, \ldots, 11\}$ can only take values which are multiples of 2 when SS/PBCH subcarrier spacing is 120kHz and values which are multiples of 4 when SS/PBCH subcarrier spacing is 240kHz. Computing of $SSB_{CRB}^{offset}$ and $SSB_{sc}^{offset}$ using $k_{SSB}$, and $N_{CRB}^{SSB}$ can be done as, $SSB_{CRB}^{offset} = \lfloor \frac{\Delta f_{CRB} * N_{CRB}^{SSB}}{\Delta f_{SSB}} \rfloor$ and $SSB_{sc}^{offset} = \frac{k_{SSB} * \Delta f_{CRB}}{\Delta f_{SSB}} + mod \left( \frac{\Delta f_{CRB} * N_{CRB}^{SSB}}{\Delta f_{SSB}} * N_{SC}^{RB}, N_{SC}^{RB} \right)$, where $\Delta f_{CRB}$ and $\Delta f_{SSB}$ are SCS of carrier and SS/PBCH respectively. Note, unequal tone amplitudes between different SCS are illustrated in Figure 5 only to avoid clutter and need not be the case in practice.

## C. SS/PBCH BLOCK
In order to provide enough deployment flexibility for NR, the number of NR physical-layer cell identities (PCIDs) is extended to 1008 (504 in LTE). Each NR-cell ID can be jointly represented by a PSS/SSS. The SS/PBCH block arrangement is shown in Figure 6. The PSSs consist of three frequency-domain-based binary phase shift keying (BPSK) m-sequences with length-127, and the SSSs correspond to m-sequences of length-127 picked from 336 m-sequences. Both PSS and SSS signals are mapped onto 127 contiguous subcarriers. With very good cross-correlation properties of m-sequences, NR SSs significantly outperform LTE SSs in terms of both PCID detection probability and false detection probability in the cases of initial and non-initial acquisition, respectively, as shown in [11]. For each SS/PBCH block, the PSS, SSS, and PBCH share the same single antenna port. It should be noted that the physical beams applied to an SS/PBCH block are transparent to the UE since the latter only sees the equivalent SSs and PBCH signal after potential precoding and/or beamforming operations that are up to the network implementation. The unique physical-layer cell ID is given by (see section 7.4.2 of [3]),

$$N_{ID}^{cell} = 3N_{ID}^{(1)} + N_{ID}^{(2)},$$

where $N_{ID}^{(1)} \in \{0, 1, \ldots, 335\}$ and $N_{ID}^{(2)} \in \{0, 1, 2\}$. $N_{ID}^{(2)}$ is carried by PSS, whereas $N_{ID}^{(1)}$ is carried by SSS. PSS is a frequency domain-based pure BPSK M-sequence with 1 generator polynomial ($g(x) = x^7 + x^4 + 1$) and 3 cyclic shifts in frequency domain ($43N_{ID}^{(2)} = \{0, 43, 86\}$). The SSS sequence is generated using two generator polynomials with cyclic shifts according to cell IDs $N_{ID}^{(1)}$ and $N_{ID}^{(2)}$. For more details (for implementation) on PSS/SSS sequence generation refer to section 7.4.2.2.1 and 7.4.2.3.1 of [3] respectively. The PBCH REs maps to 240 subcarriers in frequency and in time spans over 2 full symbols and an additional 8 RBs on the SSS symbol. PBCH contains PBCH data REs and PBCH DMRS REs. Energy Per Resource Element (EPRE) between PBCH-DMRS and PBCH-data shall be equal [3]. PBCH DMRS mapping will be frequency-first, time-second in increasing frequency order. Also, physical-layer cell ID based frequency shift is used for PBCH-DMRS RE locations (see table 7.4.3.1-1 of [3]). The 3 bits of SS block index are carried by changing DMRS sequence within each 5ms period, half-frame information is also provided for max $L = 4$, with the remaining bits of the timing information carried explicitly in the PBCH payload.

Note that the REs that are not used for SS/PBCH block in any data RB that partially or fully contain SS/PBCH block REs are transmitted with zero power and other PHY channels are rate matched around such PRBs. On the PDSCH carrying RMSI and the corresponding PDCCH CORESET, no SS/PBCH block is transmitted in the allocated resources. When the SS/PBCH and PDSCH are scheduled in the same symbols, DMRS of data and SS/PBCH can be in the same
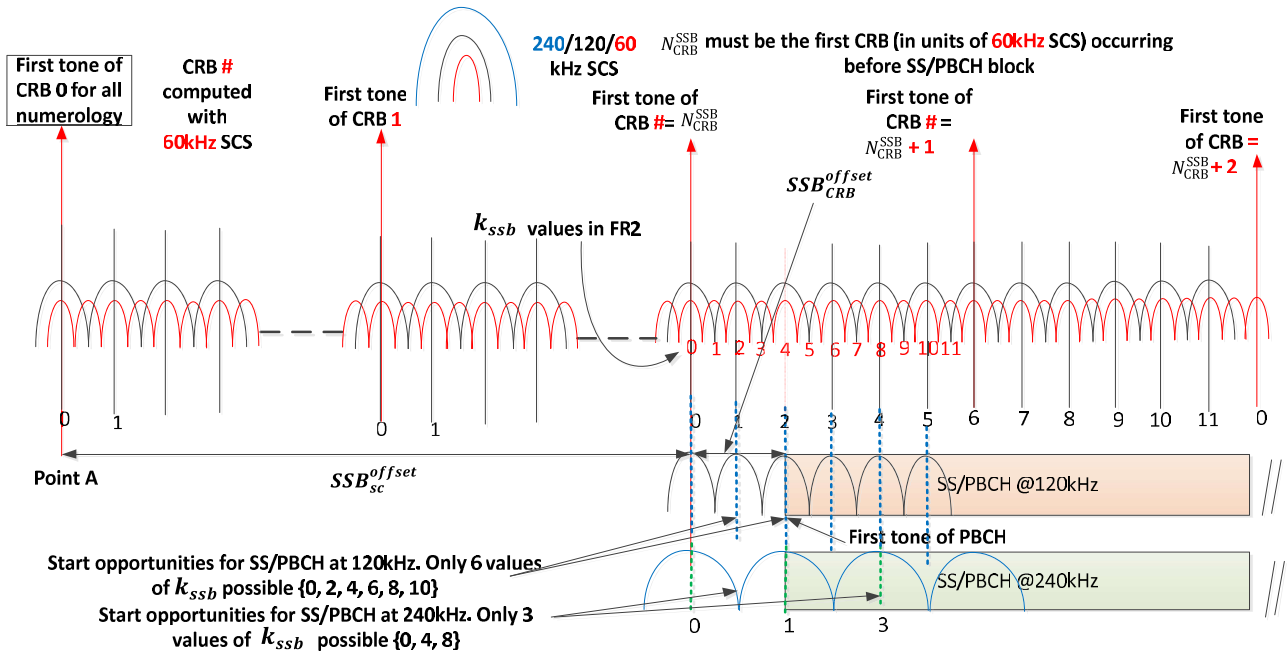
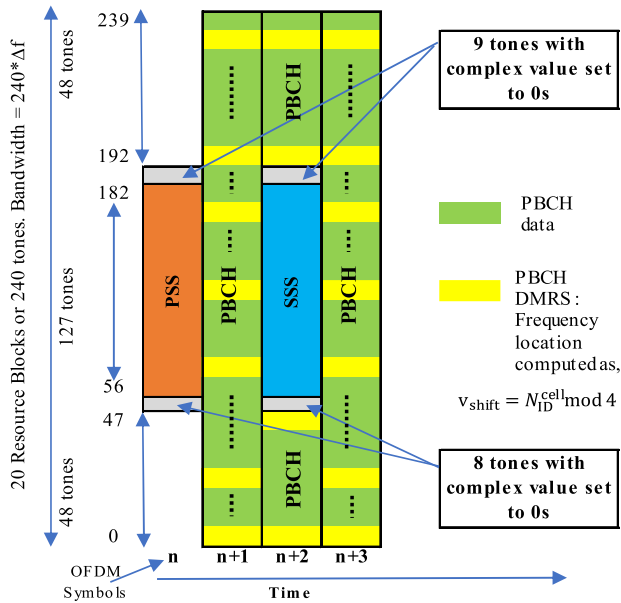**FIGURE 5.** CRB and subcarrier offset with different numerology in FR2.



**FIGURE 6.** SS/PBCH block resource arrangement.

symbol, provided DMRS of data and SS/PBCH are not overlapping in the frequency domain, spatially quasi co-located (QCL'd) and have the same SCS (see section 10.1 of [3] and section 5.1.6.2 of [9]).

### D. PBCH PAYLOAD

The PBCH payload size is 32 bits and is contained within the SS/PBCH command. The PBCH payload consists of three parts, CHOICE bit (1bit), MIB payload or the MIB
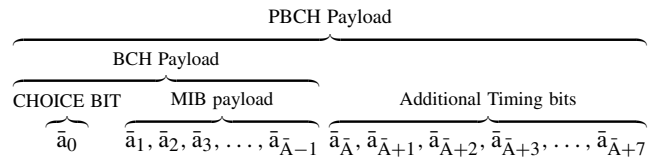
information element (IE) consisting of 23 bits (shown below in red font) defined in [S4] and the extra 8 bits related to additional timing information (see section 7.1.1 of [3]). The CHOICE bit along with the MIB payload is also known as the BCH payload. Note that the "CHOICE Bit" (see section A.3.2 of [S4]) is not part of the MIB but is part of the BCH message which includes the CHOICE bit and the MIB payload.

```
MIB ::=                       SEQUENCE {
systemFrameNumber             BIT STRING (SIZE (6)), → 6 bits
subCarrierSpacingCommon       ENUMERATED {scs15or60, scs30or120}, → 1 bit
ssb-SubcarrierOffset          INTEGER (0..15), → 4 bits
dmrs-TypeA-Position           ENUMERATED {pos2, pos3}, → 1 bit
pdcch-ConfigSIB1              PDCCH-ConfigSIB1, → 8 bits
cellBarred                    ENUMERATED {barred, notBarred}, → 1 bit
intraFreqReselection          ENUMERATED {allowed, notAllowed}, → 1 bit
spare                         BIT STRING (SIZE (1)) → 1 bit
}
```

Note that the PBCH payload bits (denoted below with the same notation as in section 7.1.1 of [3])

PBCH Payload

BCH Payload

| CHOICE BIT | MIB payload | Additional Timing bits |
|---|---|---|
| $\bar{a}_0$ | $\bar{a}_1, \bar{a}_2, \bar{a}_3, \ldots, \bar{a}_{\bar{A}-1}$ | $\bar{a}_{\bar{A}}, \bar{a}_{\bar{A}+1}, \bar{a}_{\bar{A}+2}, \bar{a}_{\bar{A}+3}, \ldots, \bar{a}_{\bar{A}+7}$ |

must be interleaved as defined in section 7.1.1 of [3], using the interleaver pattern defined in Table 7.1.1-1 of [3]. PBCH payload is scrambled (1st scrambling) before polar encoding as per the method defined in section 7.1.2 of [3]. Note that the scrambling depends on fields that are already sent in the PBCH command ($N_{ID}^{Cell}$, ssbIndex) and header (SFN). The scrambling sequence for the additional timing bits is 0.

Note that after the interleaving process, the position of the additional timing bits will change according to the interleaver pattern and care should to be taken to set only the scrambling bits to zero which correspond to the additional timing bits.

## III. OFDM SIGNAL GENERATION

In Figure 2, the spectrum allocation available for a given carrier for various subcarrier spacings with respect to reference *Point A* was shown. The common RB numbering in Figure 2 (denoted as CRB in [3]) is for the whole carrier. The first subcarrier of the common RB of different numerologies coincide at a reference point called *Point A* (see section 4.4.4.2 of [3]). Different bandwidth parts (either for uplink or downlink) can be defined by the network using different sub-carrier spacings (i.e., with $\Delta f$, $2\Delta f$, etc.). Irrespective of the different bandwidth parts the OFDM signal generation equation remains essentially common (with appropriate subcarrier-based scaling for parameters involved) for a given carrier center frequency. For successful demodulation on any bandwidth part, a phase pre-compensation is applied for all channels (except PRACH). The OFDM signal generation is described below. The baseband OFDM signal (dropping antenna port $p$ notation for convenience) in given by (section 5.3 of [3])

$$s_l^\mu(t) = \sum_{k=0}^{N_{grid}^{size,\mu}N_{SC}^{RB}-1} \alpha_{k,l}$$
$$\times e^{j2\pi\left(k+k_0^\mu-N_{grid}^{size,\mu}N_{SC}^{RB}/2\right)\Delta f\left(t-T_{CP,l}^\mu-t_{start,l}^\mu\right)} \quad (1)$$

with $T_{CP,l}^\mu = N_{CP,l}^\mu T_c$ being the duration of CP, $t_{start,l}^\mu \le t < t_{start,l}^\mu + \left(N_u^\mu + N_{cp,l}^\mu\right)T_C$ is the transmission time range of symbol $l$, with $N_u^\mu$ and $N_{cp,l}^\mu$ being the symbol and CP sizes respectively; $t_{start,l}^\mu$ is the symbol start time, as defined in [3]; $\Delta f$ and $\mu$ are the subcarrier spacing and subcarrier spacing configuration respectively, defined in section 4.2 of [3]; $\alpha_{k,l}$ is the $l^{th}$ transmitted data symbol on subcarrier index $k$; $k_0^\mu$ is a term that enables single carrier frequency for all numerologies

$$k_0^\mu = \left(N_{grid}^{start,\mu} + N_{grid}^{size,\mu}/2\right)N_{sc}^{RB}$$
$$- \left(N_{grid}^{start,\mu_0} + N_{grid}^{size,\mu_0}/2\right)N_{sc}^{RB}2^{\mu_0-\mu} \quad (2)$$

In [3], $\mu_0$ is the largest $\mu$ value among the subcarrier spacing configurations provided to the UE for this carrier.

### A. PHASE RESET AT SYMBOL BOUNDARIES: DOWNLINK RECEPTION OF SS-PBCH/RMSI/BWP

During initial access UE will not know the downlink center frequency and it may not be the same as the center frequency of SS/PBCH block and RMSI. Similarly, when the UE is configured to receive on a bandwidth part (BWP), there could mismatch in frequencies used at gNB and UE. The mismatch in center frequencies at transmitter and receiver during initial access is illustrated in Figure 7. This is handled at the gNB transmitter/UE receiver by resetting phase at OFDM symbol boundaries at the RF center frequency. This phase reset at the
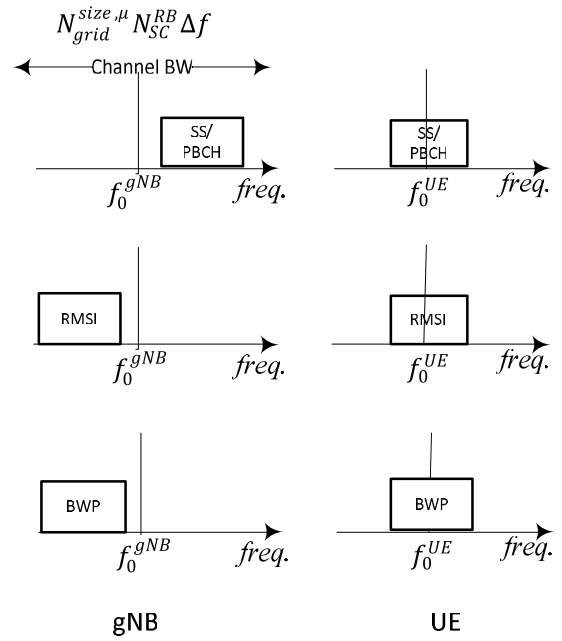


**FIGURE 7.** Center frequency mismatches at gNB and UE.

beginning of every symbol is described in the up-conversion related parts of the specifications (section 5.4 for [3]). The implementation is easier to perform at the baseband rather than RF. To understand this, consider the baseband OFDM signal (dropping antenna port $p$ notation for convenience) in section 5.3 of [3].

$$s_l^\mu(t) = \sum_{k=0}^{N_{grid}^{size,\mu}N_{SC}^{RB}-1} \alpha_{k,l}$$
$$\times e^{j2\pi\left(k+k_0^\mu-N_{grid}^{size,\mu}N_{SC}^{RB}/2\right)\Delta f\left(t-T_{CP,l}^\mu-t_{start,l}^\mu\right)} \quad (3)$$

with $T_{CP,l}^\mu = N_{CP,l}^\mu T_c$ being the duration of CP, $t_{start,l}^\mu \le t < t_{start,l}^\mu + \left(N_u^\mu + N_{cp,l}^\mu\right)T_C$ is the transmission time range of symbol $l$, with $N_u^\mu$ and $N_{cp,l}^\mu$ being the symbol and CP sizes respectively; $T_C$ is the basic unit of sample duration; $t_{start,l}^\mu$ is the symbol start time, as defined in [3]; $\Delta f$ and $\mu$ are the subcarrier spacing and subcarrier spacing configuration respectively, defined in section 4.2 of [3]; $\alpha_{k,l}$ is the $l^{th}$ transmitted data symbol on subcarrier index $k$; $k_0^\mu$ is a term that enables use of a single carrier frequency for all numerologies (see following sections). Assuming the center frequency of the gNB to be $f_0^{gNB}$, the transmitted signal is,

$$x_l(t) = e^{j2\pi f_0^{gNB}t}s_l(t)$$

Assuming the UE center frequency as $f_0^{UE}$, the received signal can be written as, $y_l(t) = e^{-j2\pi f_0^{UE}t}x_l(t)$. Expanding,

$$y_l\left(t+t_{start,l}^\mu\right)$$
$$= \overbrace{e^{j2\pi f_0^{gNB}\left(T_{CP,l}^\mu+t_{start,l}^\mu\right)}}^{gNB\ phase\ part}\overbrace{e^{-j2\pi f_0^{UE}\left(T_{CP,l}^\mu+t_{start,l}^\mu\right)}}^{UE\ phase\ part}$$

$$\times \sum_{k}^{N_{grid}^{size,\mu} N_{SC}^{RB}-1} h_{k,l} a_{k,l}$$

$$\times e^{j2\pi\left(k+k_0^\mu - N_{grid}^{size,\mu} N_{SC}^{RB}/2+\Delta k\right)\Delta f\left(t-T_{CP,l}^\mu\right)} \quad (4)$$

where $\Delta k = \frac{f_0^{gNB}-f_0^{UE}}{\Delta f} + k_0^\mu - \frac{N_{grid}^{size,\mu} N_{SC}^{RB}}{2}$. Note that the center frequency offset (i.e., $f_0^{gNB} - f_0^{UE}$) is always an integer number of subcarriers. Also, $\Delta k$ is independent of $l$ and hence will not impact reception. Therefore, the impact of this center frequency offset is only the per-symbol phase rotation caused by gNB center frequency as the UE phase part in Eq. (4) can be corrected as $f_0^{UE}$ is known at the UE. The gNB part of the residual phase on every symbol can be compensated in the baseband (at gNB) by multiplying with the conjugate of the gNB part of the residual phase at the transmitter. This is,

$$s_l^\mu(t) e^{-j2\pi f_0^{gNB}(T_{CP,l}^\mu + t_{start,l}^\mu)}, \quad (5)$$

which will result in the received signal not having terms dependent on gNB center frequency. The phase compensation can also be done at the up-conversion step (as described in the spec [3]) as follows –

$$Re\left\{ s_l^\mu(t) e^{j2\pi f_0^{gNB}t} * e^{-j2\pi f_0^{gNB}\left(T_{CP,l}^\mu + t_{start,l}^\mu\right)} \right\}$$
$$= Re\left\{ s_l^\mu(t) e^{j2\pi f_0^{gNB}\left(t-T_{CP,l}^\mu - t_{start,l}^\mu\right)} \right\} \quad (6)$$

This essentially implies the phase of the RF signal is reset at symbol boundaries. This is difficult to implement in RF analog domain. The baseband signal can be pre-compensated so that there is no need for phase reset in RF. Note that, only for PRACH signal transmission, there is no common phase correction applied during the up-conversion at the transmitter (see section 5.4 of [3]) as accurate phase information may not be necessary for PRACH demodulation. Common phase correction can be implemented in the IFFT/FFT modules of transmitter/receiver respectively. This phase reset works only when the difference in the transmission and reception frequencies is a multiple of subcarrier spacing. $f_0^{gNB}$ is a multiple of 1 kHz and hence the phase terms $e^{-j2\pi f_0^{gNB}(T_{CP,l}^\mu + t_{start,l}^\mu)}$ will repeat every 1 ms (see [26]). So, it is enough to pre-compute phase terms for $2^\mu \times 14$ symbols. The subcarriers in the range

$$\left(\left(N_{BWP}^{start,\mu} - N_{grid}^{start,\mu}\right) N_{SC}^{RB}, \right.$$
$$\left. \left(N_{BWP}^{start,\mu} - N_{grid}^{start,\mu}\right) N_{SC}^{RB} + N_{BWP}^{size,\mu} N_{SC}^{RB} - 1\right)$$

is of interest, where $N_{BWP}^{start,\mu}$ and $N_{grid}^{start,\mu}$ are starting CRB of BWP and carrier grid with sub-carrier spacing $\mu$ respectively (see Figure 8). So, a smaller FFT around $\left(N_{BWP}^{start,\mu} - N_{grid}^{start,\mu}\right) N_{SC}^{RB} + N_{BWP}^{size,\mu} N_{SC}^{RB}/2 - 1$ should be sufficient. Note that the pre-compensation and IFFT operations are interchangeable. The phase reset at symbol boundaries
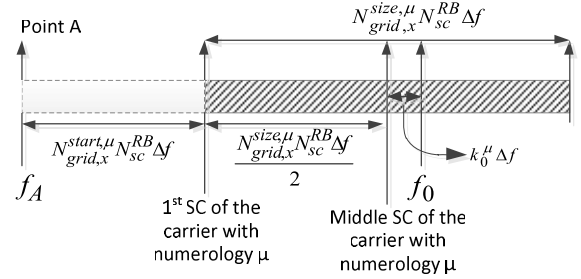


**FIGURE 8.** Relationship between $k_0^\mu$, $f_0$ and other parameters.

is useful to do the following with only the knowledge of the corresponding BWP parameters. 1) UE can receive SS-PBCH, RMSI or data on a BWP 2) UE can transmit on any BWP. After downlink synchronization, the center frequencies of gNB and UE will be the same, i.e., $f_0^{gNB} = f_0^{UE} = f_0$ and a single $f_0$ is used to transmit and receive on a given BWP. Users within a given BWP can center their FFT at the middle of their configured BWP, and while upconverting use a frequency offset to the carrier center frequency $f_0$. The frequency $f_0^{BWP}$ to be used during up-conversion is given by

$$f_0^{BWP} = f_0 - \left( N_{grid}^{size,\mu} N_{SC}^{RB}/2 - N_{BWP}^{start,\mu} N_{SC}^{RB} \right.$$
$$\left. - N_{BWP}^{size,\mu} N_{SC}^{RB}/2 + N_{grid}^{start,\mu} N_{SC}^{RB} \right)\Delta f.$$

At the gNB receiver, a corresponding phase reset must be applied at symbol boundaries in RF. Again, this is easier to do in the baseband (just like in the transmitter). The per-symbol phase correction to be applied at the receiver for OFDM symbol index $l$ is given by $e^{j\theta_l}$, where $\theta_l = 2\pi f_0\left(t_{start,l}^\mu + T_{CP,l}^\mu\right)$, where $f_0$ is the receiver center frequency in Hz. If the receiver center frequency is a multiple of 1 kHz, it can be shown that the phase correction factors $\theta_l$ defined above are periodic with a periodicity of 1ms (i.e. at most 28 unique values for $\mu = 1$, see [26]). If the receiver center frequency includes a 7.5 kHz shift when UL is shared with LTE, the periodicity is 2ms (i.e. at most 56 unique values for $\mu = 1$ [26]).

### B. FREQUENCY OFFSET PARAMETER

The locations of the RB grids of all numerologies are indicated to the UE using RRC parameters $N_{grid,x}^{start,\mu}$ and $N_{grid,x}^{size,\mu}$ [8]. The parameter $k_0^\mu$ is the subcarrier offset from the middle subcarrier of numerology $\mu$ (i.e. the $N_{grid,x}^{size,\mu} N_{sc}^{RB}/2 + 1$'th subcarrier in the $N_{grid,x}^{size,\mu} N_{sc}^{RB}$ subcarriers) to $f_0$, as illustrated in Figure 8. From Figure 8, one can write,

$$f_0 - f_{point-A} = N_{grid,x}^{start,\mu} N_{sc}^{RB} \Delta f$$
$$+ N_{grid,x}^{size,\mu} N_{sc}^{RB}/2 \times \Delta f - k_0^\mu \Delta f \quad (7)$$

Therefore, for any two numerologies $\mu$ and $\mu_0$:

$$\left( N_{grid,x}^{start,\mu_0} N_{sc}^{RB} + N_{grid,x}^{size,\mu_0} N_{sc}^{RB}/2 - k_0^{\mu_0} \right) \times 2^{\mu_0}$$
$$= \left( N_{grid,x}^{start,\mu} N_{sc}^{RB} + N_{grid,x}^{size,\mu} N_{sc}^{RB}/2 - k_0^\mu \right) \times 2^\mu. \quad (8)$$

**TABLE 1.** PRACH configuration for Frequency Range 2 (FR2).

| PRACH Config. Index | Preamble format | $n_{SFN} \bmod x = y$ | | Slot number | Starting symbol | Number of PRACH slots within a 60 kHz slot | $N_t^{RA,slot}$ number of time-domain PRACH occasions within a PRACH slot | $N_{dur}^{RA}$ PRACH duration |
|---|---|---|---|---|---|---|---|---|
| | | $x$ | $y$ | | | | | |
| 14 | A1 | 1 | 0 | 24,29,34,39 | 7 | 1 | 3 | 2 |



**FIGURE 9.** PRACH preamble for different formats with short-sequence length.

Rewriting the above equation for $k_0^\mu$, we have,

$$k_0^\mu = N_{grid,x}^{start,\mu} N_{sc}^{RB} + N_{grid,x}^{size,\mu} N_{sc}^{RB}/2$$
$$+ \left( k_0^{\mu_0} - N_{grid,x}^{start,\mu_0} N_{sc}^{RB} - N_{grid,x}^{size,\mu_0} N_{sc}^{RB}/2 \right) \times 2^{\mu_0-\mu}. \quad (9)$$

Note that $f_0$ does not have to be on the channel raster nor the center of the RF filter. The channel raster or the RF implementations do not impose any restriction to the value of $k_0^{\mu_0}$. Therefore, the value of $k_0^{\mu_0}$ can be predefined and is set to 0 i.e., $k_0^{\mu_0} = 0$. Accordingly, $k_0^\mu$ can be derived using:

$$k_0^\mu = \left( N_{grid}^{start,\mu} + N_{grid}^{size,\mu}/2 \right) N_{sc}^{RB}$$
$$- \left( N_{grid}^{start,\mu_0} + N_{grid}^{size,\mu_0}/2 \right) N_{sc}^{RB} 2^{\mu_0-\mu}. \quad (10)$$

## IV. PRACH DESIGN
In this section we will discuss PRACH channel and its design principles in 5G-NR. Two preamble formats are defined in NR, long and short preamble formats of sequence

length 839 and 139 respectively. Long formats can be configured only for sub-6GHz frequency range (FR1), whereas short formats can be configured for both sub-6 (FR1) and mmW (FR2) frequency range. Long formats option is mainly aimed towards catering for LTE re-farming and large cell scenarios [2]. In this paper, we will consider only the short preamble formats. The PRACH preamble consists of a cyclic prefix of duration $T_{CP}$ ($N_{CP}^{RA}$ samples) and sequence part of duration $T_{SEQ}$ ($N_u$ samples and with or without repetitions depending on the PRACH format) and guard duration of $T_{GP}$. Figure 9 shows the various PRACH preamble formats associated with short-sequence length, with sizes of cyclic prefix (CP), PRACH sequence, Guard duration (if any) in number of samples for the configured parameters (i.e., $\mu$, $f_s$ and starting symbol shown on the right side of Figure 9) and the bandwidth of each format. For PRACH formats with no guard duration, the CP is aggregated for the number of repetitions of the sequence(s) and appended at the beginning of the PRACH sequence(s). For PRACH formats with guard
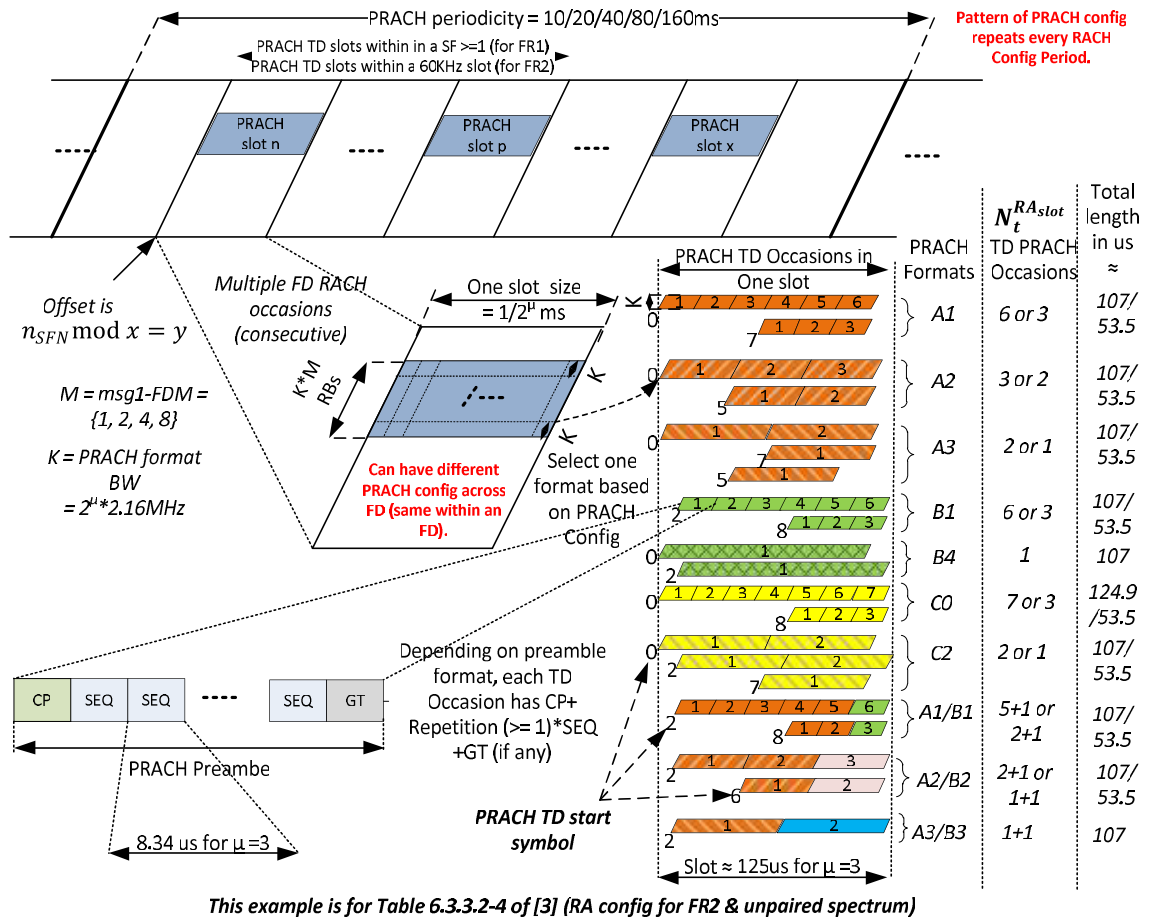
**FIGURE 10.** PRACH time frequency structure.

duration, the guard duration $T_{\text{GP}}$ extends from the end of the preamble to the next symbol boundary. The preambles for all formats always start and end at symbol boundaries within a slot (see Figure 12 in section IV-B). Also shown is the length of each preamble sequence in micro-seconds. The CP length, sequence length and total preamble length (in samples) can be calculated for short sequence length preambles using the Table 6.3.3.1-2 of [3]. The time duration of different preamble components (sequence, CP, guard etc) for different preamble formats shown in Figure 9 are with subcarrier spacing of $\Delta f_{RA} = 120$kHz ($\mu = 3$). Bandwidth for a frequency domain occasion with short sequence and SCS of 120kHz can be calculated as $BW = \left\lceil \frac{139}{12} \right\rceil \times 12$ tones $\times 120$kHz $= 17.28$MHz.

## A. PRACH TIME/FREQUENCY STRUCTURE

Within a cell, preamble transmission can take place within a configurable subset of slots (denoted as the PRACH slots) that repeats every PRACH configuration period as shown in Figure 10. The PRACH configuration period is given by the parameter $x$ in Table 6.3.3.2-4 of [3] for FR2. PRACH periodicity can be configured to range from 10 ms up to 160 ms. A configurable set of PRACH slots are present

within the PRACH period. For a given SFN, a PRACH slot can be present only when $n_{SFN} \bmod x = y$. Further, for a given SFN, where PRACH slots can be present (i.e., when $n_{SFN} \bmod x = y$), PRACH can be only be on slots given by 'Slot Number' column in Table 6.3.3.2-4 of [3] for FR2. As an example, let SFN = 1 (i.e., 2nd frame) and let PRACH config index = 14 (see Table 1). Then, for PRACH config index = 14, the parameters $x = 1$ and $y = 0$ (using Table 6.3.3.2-4 of [3] of FR2), shown below. PRACH slots are on slot numbers 24,29,34,39 (using Table 6.3.3.2-4 of [3] of FR2), from the snippet shown in Table 1. Section 2 of [24] has more information on PRACH slot in a frame based on subcarrier spacing. Within any given PRACH slot (see Figure 10), multiple PRACH occasions can exist consecutively in time and frequency. Utilization of multiple time & frequency resources is towards yielding NR-PRACH capacity as large as LTE [29]. This is because PRACH capacity would be limited compared to LTE with large subcarrier spacing and short sequence lengths.

Details on time domain occasions within a PRACH slot is shown in Figure 10. There can be multiple frequency domain PRACH occasions jointly covering $K * M$ consecutive resource blocks, where $K$ is the preamble bandwidth
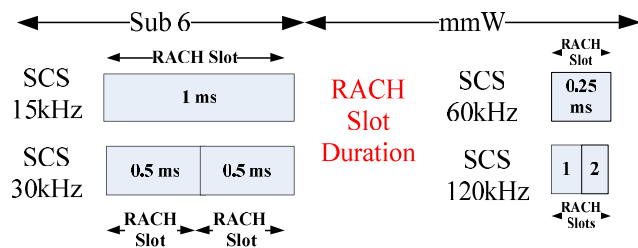
**FIGURE 11.** PRACH slot definitions for different $\mu$.

measured in number of resource blocks and $M$ is the number of frequency-domain PRACH occasions defined by the higher layer parameter *msg1-FDM* with $M \in \{1, \cdots, 8\}$. PRACH configuration can be different across frequency domain occasions, but within a given a frequency domain occasion, the PRACH configuration will same across all time-domain occasions.

## B. DEFINITION OF PRACH SLOT NUMBER

Column 'Slot Number' in Table 6.3.3.2-4 of [3] is defined in terms of 60kHz SCS for FR2. Essentially, the number of PRACH slots is defined as the number of PRACH slots within a subframe for FR1 ($\mu = 15, 30$ kHz) and the number of PRACH slots within a 60kHz slot for FR2 ($\mu = 60, 120$ kHz) as shown in Figure 11. Therefore, the column 'Slot Number' in Table 6.3.3.2-4 of [3] is always between 0 to 39 for FR2. For a given PRACH config, when the number of PRACH slots within a 60kHz is specified as 1 in Table 6.3.3.2-4 of [3] and when PRACH subcarrier spacing is 120kHz (with 2 slots in a 60kHz), PRACH is always transmitted on the 2nd slot of 120kHz SCS (see section 5.3.2 of [3]). For the example PRACH configuration in Table 1, within the allowable slots numbers 24,29,34 and 39 (or slots {48,49}, {58,59}, {68,69} and {78,79} in terms of 120kHz SCS), PRACH can be transmitted only in the 2nd slot corresponding to 120kHz numerology, i.e., slots 49, 59, 69 and 79 slots of 120kHz. For a given preamble type, corresponding to a certain preamble bandwidth, the overall available time/frequency PRACH resource within a cell can now be described as follows (see illustration in Figure 10). Within a given frequency domain PRACH occasion, there can be multiple TD occasions defined by the parameter $N_t^{RA_{slot}}$ given in Table 6.3.3.2-4 in [3]. The duration of each TD occasion is given by the parameter $N_{dur}^{RA}$ and is in terms of PUSCH symbols. Within each TD occasion the configured PRACH preamble is present, including CP, sequence(s) and guard (if any) of durations $T_{CP}$, $T_{SEQ}$ and $T_{GT}$ respectively, as shown in Figure 10. Note that all TD occasions are continuous in time (i.e., no gaps between TD occasions). Alignment of PRACH symbols for different formats with OFDM symbol boundaries is shown in Figure 12. For a given PRACH format/configuration, the time domain occasion can start at different symbols as specified by the "starting symbol" (or $l_0$ in section 5.3.2 of [3]) column of Table 6.3.3.2-4 in [3]. Symbol start period of 2 was chosen to

accommodate PDCCH on first two symbols (see section 2.1 of [25]). Start symbol 6 and 8 was chosen to avoid DL to UL interference. A significant concern was the transmission point (TRP) to TRP, or DL-to-UL interference between PRACH and a preceding PDCCH transmitted in a gap at the beginning of the slot [32]. If the preamble format specified in Tables 6.3.3.2-2 to 6.3.3.2-4 of [3] is A1/B1, A2/B2 or A3/B3, then only the last TD occasion will have the preamble format of B1, B2 or B3 respectively (see section 5.3.2 of [3]). Note that, formats B2 and B3 are only supported in combination with A2 and A3 respectively, i.e., B2 and B3 cannot be configured by themselves. Also, with Ax/Bx format, supporting Bx seems mandatory(see [30]), although the 3GPP specification doesn't explicitly state this. Here, Ax/Bx corresponds to A1/B1, A2/B2 or B3/B3 short format pairs.

For preamble format A, guard duration is not explicitly defined. Since Ax doesn't have a guard band, Bx (which has a guard band) was appended to Ax, when Ax/Bx is configured. But again, having no Bx would have acted as a guard band for the last time domain occasion of Ax, but Bx was chosen instead [31] of defining a guard period for the last time domain occasion of Ax. The CP sizes of Ax are larger than Bx. Given this, for example, consider a scenario where, UE-1 is configured to use A2 format and UE-2 is configured to use B2 format. Then if UE1 propagation delay is greater than B2 CP, then it may interfere with UE-2s PRACH (if UE-2 is close to gNB). The medium access control (MAC) scheduler should take care to avoid this scenario. Further, PRACH is supposed to work at low SNR during interference, so UE-2 performance may not be significantly impacted (see [30]). One benefit of having PRACH preamble start and end at the user data OFDM symbols (as shown in Figure 12) is the negligible inter-carrier interference (that too for the first and the last OFDM symbols) if the preamble is delayed. Note that format C2 has the largest guard period and CP size across all formats as it was intended for larger cell coverage (see cell dimensioning in section 4.C.2. Also, RAN4 performance evaluations will be only for formats are A1, A2, A3, B4, C0 and C2, see [6] and [23]. Coverages shown in Table 2 of section 4.C, shows that support of formats A1, A2, A3 and A3/B3 may suffice for small cells. Support of mixed format of format A and format B was agreed, in order to avoid the inter-symbol interference to the following uplink/downlink data receiving/transmitting at gNB/UE due to the zero-guard time of preamble format A (see [31]) and may need to be supported for a small cell scenario.

## C. PRACH CHANNEL DESIGN

As discussed in section 2.2.2.1, NR PRACH short sequence formats are defined with different CP durations, and sequence repetitions to cater for different size cells and PRACH capacity. In this section, brief details are provided on PRACH preamble generation/properties and cell sizes/cyclic-shift dimensioning. Understanding PRACH preambles generation/properties will be useful towards understanding the
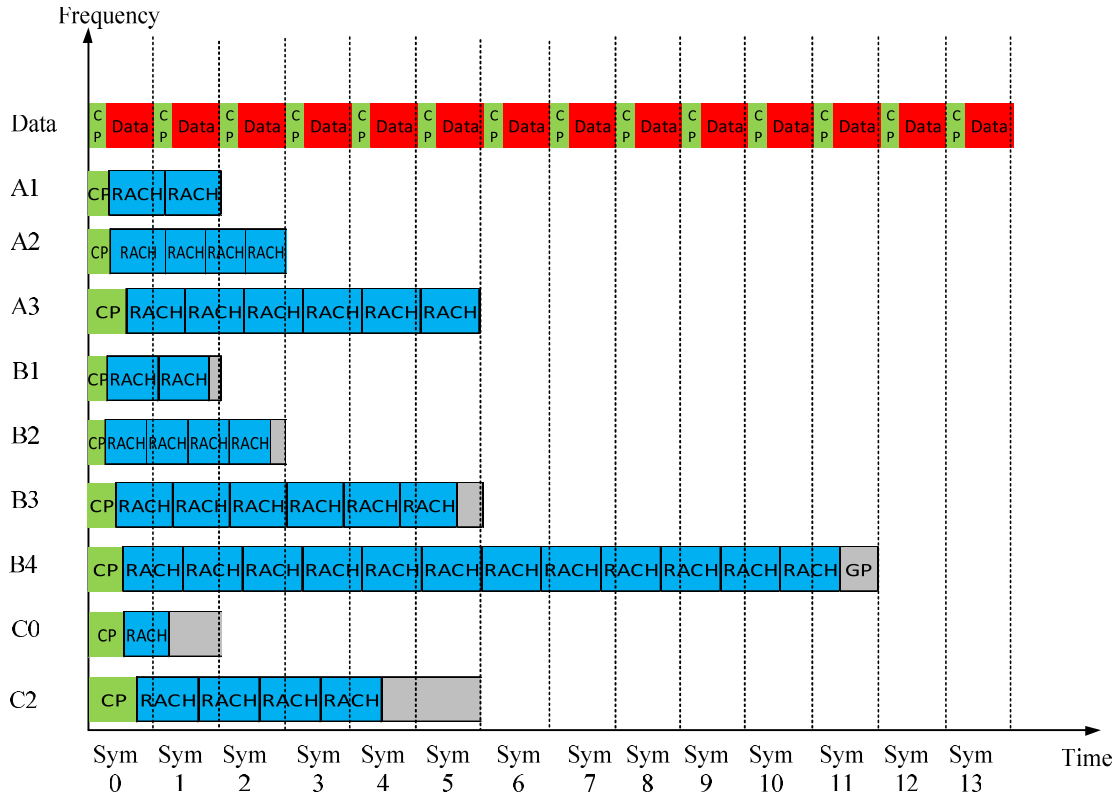
**FIGURE 12.** Short preamble format timelines in 5G NR.

PRACH receiver detection/estimation. Understanding cell sizes/cyclic-shift dimensioning for all PRACH formats will be useful towards analysing receiver processing complexity for any given PRACH format and defining gNB requirements.

The basic PRACH preamble sequences (of duration $T_{SEQ}$ and number of tones $L_{RA}$) are Zadoff-Chu (ZC) sequences generated using a given root sequence and a given cyclic shift. A gNB configures the set of preamble sequences (with a maximum of up to 64 preambles) the UE can use, and UE will select one preamble (randomly out of the 64 preambles) for transmitting *msg1* (or PRACH preamble).

A PRACH receiver objective is to detect the transmitted preamble at the correct root sequence and cyclic shift and estimate the timing offset (propagation delay) for the given UE. The generation and transmission of preamble is briefly described below. A ZC sequence can be generated in time-domain (TD), using a physical root sequence $u$ as $x_u(n) = e^{-j\frac{\pi un(n+1)}{L_{RA}}}$, $n = 0, 1, \ldots, L_{RA} - 1$, where $L_{RA}$ is the sequence length with $u \in \{0, 1, \ldots, L_{RA}-1\}$. For short sequence preamble formats $L_{RA} = 139$. The gNB configures the UE to use a start logical root sequence $i$ (higher layer parameter *prach-RootSequenceIndex*), which is used to derive the start physical root sequence $u$, using Table 6.3.3.1-4 of [3] for FR2. A cyclic shifted version (with cyclic shift value of $C_v$) of the ZC-TD signal can be obtained as $x_{u,v}(n) = x_u((n + C_v) \mod L_{RA})$. For unrestricted set

(i.e., with low or no Doppler), the cyclic shift is given by,

$$C_v = \begin{cases} vN_{CS} & v = 0, 1, \ldots, \left\lfloor \frac{L_{RA}}{N_{CS}} \right\rfloor - 1, N_{CS} \neq 0 \\ 0 & N_{CS} = 0 \end{cases} \quad (11)$$

The parameter $N_{cs}$ is configured by the gNB which is derived from the higher layer parameter *zeroCorrelationZoneConfig* using Table 6.3.3.1-7 of [3] for FR2. The $N_{CS}$ parameter specifies how many cyclic shifts can be used within a given root sequence. Using the start physical root sequence and $N_{CS}$, the UE generates 64 ZC sequences (or preambles) for each time-frequency PRACH occasion, enumerated in first increasing order of cyclic shifts $C_v$ of a logical root sequence, and then in increasing order of the logical root sequence index (section 6.3.3.1 of [3]). A frequency domain (FD) version of the sequence is generated as $y_{u,v}(n) = \sum_{m=0}^{L_{RA}-1} x_{u,v}(m) \cdot e^{-j\frac{2\pi mn}{L_{RA}}}$. All 64 preambles can be generated using a single root sequence or using multiple root sequences depending on the sequence length $L_{RA}$ and the cyclic shift parameter $N_{CS}$. An example for each scenario is illustrated in Figure 13 and Figure 14 for $L_{RA} = 139$ (short sequence).

### 1) ZC PROPERTIES FOR PREAMBLE DETECTION

Specifically, two properties of the ZC sequences (see chapter 7 of [20] for all properties of ZC sequences) are useful at the receiver for detection and timing estimation
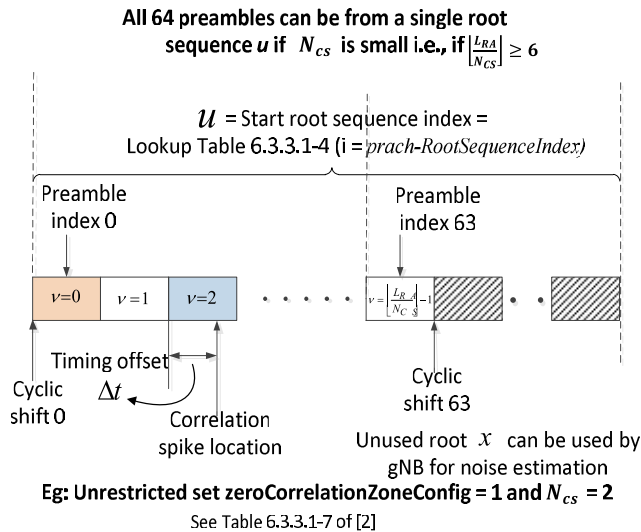
**All 64 preambles can be from a single root sequence $u$ if $N_{cs}$ is small i.e., if $\left\lfloor \frac{L_{RA}}{N_{CS}} \right\rfloor \geq 6$**

$\mathcal{U}$ = Start root sequence index =
Lookup Table 6.3.3.1-4 (i = *prach-RootSequenceIndex*)

Preamble index 0

Preamble index 63

$v=0$  $v=1$  $v=2$  · · · · · ·  $v = \left\lfloor \frac{L_R}{N_C} \right\rfloor -1$

Timing offset

Cyclic shift 0  $\Delta t$  Correlation spike location

Cyclic shift 63

Unused root $x$ can be used by gNB for noise estimation

Eg: Unrestricted set zeroCorrelationZoneConfig = 1 and $N_{cs}$ = 2

See Table 6.3.1-7 of [2]

**FIGURE 13.** Generating preambles from a single root sequence for $L_{RA} = 139$ (short sequence).

(for unrestricted sets). First, the normalized cross-correlation between two unique ZC sequences (i.e., ZC sequences generated with two different root sequences) will be low and equal to $\frac{1}{\sqrt{L_{RA}}}$. Second property is that the cyclic shifts of a ZC sequence (i.e., generated with a given root sequence) are orthogonal (i.e., zero cross-correlation) to each other. Note that the orthogonality between cyclic shifts is retained at the receiver side only if the relative cyclic shift between two sequences is larger than any difference in their respective received timing. Therefore, in practice only a subset of the cyclic shifts can be used to generate orthogonal preambles,

where the number of available shifts depends on the maximum timing uncertainty to be considered (depends on cell size). In general, for small cell sizes a relatively large number of cyclic shifts are available compared to larger cell sizes. Table 2 shows the maximum cell radius for different formats of both long and short-sequence length PRACH preambles for all values of $\mu$. The supported cell size is determined by the minimum of the zero-correlation zone length $N_{CS}$ and the guard period length $N_{GP}$. For low Doppler scenarios, all possible cyclic shifts are allowed and are labelled as Unrestricted Sets. In the case of high Doppler scenarios, some of the cyclic shifts are not allowed. This is because of a property of ZC sequences according to which energy transmitted on a given cyclic shift will appear at other cyclic shifts depending upon the root sequence and the sequence length. These cyclic shifts are not considered in forming the preamble sets and are labelled as "Restricted Sets". For detection of preambles from restricted sets, the correlation energy of these "co-cyclic shifts" will also need to be accumulated. Restricted sets are not applicable for frequency range 2, i.e., FR2 in 5G-NR.

The parameter $N_{CS}$ indicates the width of the "zero-correlation zone", thus providing larger or smaller "zones" in terms of timing error for which orthogonality (i.e., zero correlation) is retained. The set of cyclic shifts for a sequence are partitioned into groups of $N_{CS}$ shifts per preamble index. Essentially, the gNB receiver looks for a strong correlation with one of the root sequences. Location of the spike (i.e., which cyclic shift) determines the preamble index (within which $N_{CS}$ group it shows up in) and the timing (where in the $N_{CS}$ group is shows up). Note that the gNB is aware of the start root sequence and number of root sequences used (depending on the parameter $N_{CS}$ gNB has

**64 preambles can be from different root sequences $u$ if $N_{CS}$ is large i.e., if $\left\lfloor \frac{L_{RA}}{N_{CS}} \right\rfloor < 64$**

Preamble index 0

$v=0$  $v=1$  $v=2$  $v=6$

$\mathcal{U}$ = Start root sequence index =
Lookup Table 6.3.3.1-4
(i = *prach-RootSequenceIndex*)

$u+1$

$v=0$  $v=1$  $v=2$  $v=6$

Cyclic shift 0

Timing offset

Cyclic shift 7  $\Delta t$

Preamble index 63

$u+8$

$v=0$

Correlation spike location

Cyclic shift 63

Unused root $x$ can be used by gNB for noise estimation

**Eg: Unrestricted set zeroCorrelationZoneConfig = 10 and $N_{CS} = 19$**

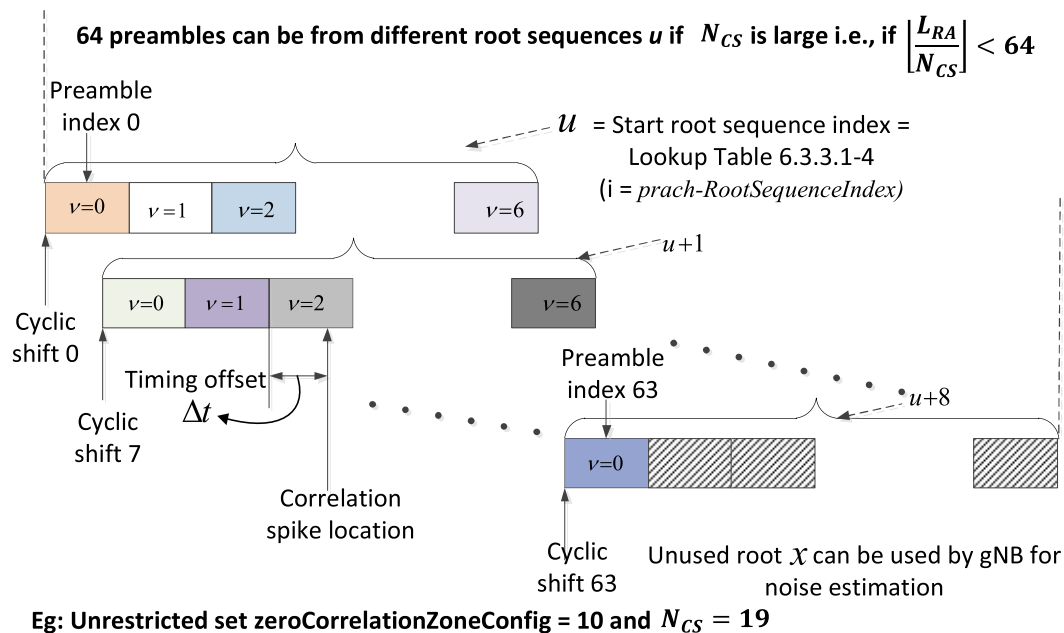**FIGURE 14.** Generating preambles from different root sequences for $L_{RA} = 139$ (short sequence).

**TABLE 2.** NR PRACH Cell dimensioning.

| | | PRACH format | Number of reps. | Tcp | Tseq | TGP | Path profile (Ts) | Path profile (us) | Use case | Upper bound on $N_{CS}$ | Quantized $N_{CS}$ less than CP | Number of cylic shifts | Number of root sequences | Maximum radius (m) for 15 kHz SCS | Maximum radius (m) for 30 kHz SCS | Maximum radius (m) for 60 kHz SCS | Maximum radius (m) for 120 kHz SCS |
|---|---|---|---|---|---|---|---|---|---|---|---|---|---|---|---|---|---|
| Short Sequence | | A1 | 2 | 288 | 4096 | 0 | 96 | 3.13 | Small cell | 19.54688 | 19 | 7 | 10 | 939 | 448.703237 | 224.35162 | 112.175809 |
| | | A2 | 4 | 576 | 8192 | 0 | 144 | 4.69 | Normal cell | 39.09375 | 34 | 4 | 16 | 2110 | 871.271583 | 435.63579 | 217.817896 |
| | | A3 | 6 | 864 | 12288 | 0 | 144 | 4.69 | Normal cell | 58.64063 | 46 | 3 | 22 | 3517 | 1302.92626 | 651.46313 | 325.731565 |
| | | B1 | 2 | 216 | 4096 | 72 | 96 | 3.13 | Small cell | 14.66016 | 13 | 10 | 7 | 586 | 232.875899 | 116.43795 | 58.2189748 |
| | | B2 | 4 | 360 | 8192 | 216 | 144 | 4.69 | Normal cell | 24.43359 | 23 | 6 | 11 | 1055 | 475.588129 | 237.79406 | 118.897032 |
| | | B3 | 6 | 504 | 12288 | 360 | 144 | 4.69 | Normal cell | 34.20703 | 34 | 4 | 16 | 1758 | 871.271583 | 435.63579 | 217.817896 |
| | | B4 | 12 | 936 | 24576 | 792 | 144 | 4.69 | Normal cell | 63.52734 | 46 | 3 | 22 | 3869 | 1302.92626 | 651.46313 | 325.731565 |
| | | C0 | 1 | 1240 | 2048 | 1096 | 144 | 4.69 | Normal cell | 84.16016 | 69 | 2 | 32 | 5354 | 2130.26439 | 1065.1322 | 532.566097 |
| | | C2 | 4 | 2048 | 8192 | 2916 | 144 | 4.69 | Normal cell | 139 | 139 | 1 | 64 | 9301 | 4648.25 | 2324.125 | 1162.0625 |
| | | | | | | | | | | | | | | Maximum radius (m) for Long Formats | | | |
| Long Sequence | 1.25k Hz SCS | 0 | 1 | 3168 | 24576 | 2976 | 192 | 6.25 | LTE refarming | 108.1523 | 93 | 9 | 8 | 12364.04946 | | | |
| | | 1 | 2 | 21024 | 49152 | 21904 | 512 | 16.67 | Large cell (<100km) | 717.7383 | 419 | 2 | 32 | 57427.98629 | | | |
| | | 2 | 4 | 4688 | 98304 | 4528 | 192 | 6.5 | Coverage enh. | 160.0436 | 167 | 5 | 13 | 22910.57807 | | | |
| | 5 kHz SCS | 3 | 4 | 3168 | 24576 | 2976 | 192 | 6.25 | High speed case | 432.6094 | 439 | 1 | 64 | 14759.75864 | | | |

configured) and hence needs to do sequence matching (or correlation) for only the configured roots sequences. At the receiver, the received signal is sequence matched with a set of ZC-sequences starting from the starting root (and up to number of roots required) and typically filtered using an IFFT for preamble detection and timing estimation (see section 5 and Figure 5.1 for more details). The IFFT filtering operation will cover for all the cyclic shifts used within the given root sequence, i.e., preamble transmitted with a given root sequence and any cyclic shift within can be detected with a single IFFT. Therefore, the receiver complexity scales only with the number of root sequences used. The details on receiver complexity is provided in section 6.A.

### 2) CELL DIMENSIONING
The cell radius, number of cyclic shifts and number of root sequences required to generate 64 preambles can be computed as below. Parameters $T_{cp}$, $T_{seq}$ and path profile values (in samples) in Table 2 are assuming 15kHz SCS (see Table 6.3.3.1 − 2 of [3] and scaled accordingly for different SCS. Maximum radius in Table 2 for different SCS is computed as follows. First, compute $N_{CS}$ as follows. **Step 1:** First compute $N'_{CS} = \frac{N^{RA}_{Cp}}{(2048)} \times L_{RA}$. Using $N'_{CS}$, find the quantized value of $N_{CS}$ using Table 6.3.3.1 − 7 of [3] for F R2. E.g., for A1 format, $N'_{CS}$ will be $(288/2048)*139 = 19.54$ which will be quantized to 19. **Step 2:** Compute number of cyclic shifts required as $C_v = \left\lfloor \frac{L_{RA}}{N_{CS}} \right\rfloor$. E.g., for A1 format, this will be $C_v = \left\lfloor \frac{139}{19} \right\rfloor = 7$.

**Step 3:** Compute the number of root sequences required to generate 64 preambles as, $\left\lceil \frac{64}{Cv} \right\rceil$. E.g., for A1 format, this will be $\left\lceil \frac{64}{7} \right\rceil = 10$. **Step 4:** The cell radius (see [20]) can be calculated as Cell Radius $= \left( \frac{N_{CS}}{\Delta f_{RA} L_{RA}} - \frac{\tau_d}{2^\mu} \right) \times \frac{300}{2}$ (in meters). Here, $\tau_d$ is the delay spread equal to the PUSCH CP size (144 $T_s$ or 4.69 $\mu s$@15kHz).

The maximum cell radius, number of cyclic shifts and root sequences required for all NR PRACH formats are shown in Table 2 when un-restricted sets are used. Preamble indices not used for Contention based Random Access (CBRA) in a PRACH occasion can be reserved for Contention Free Random Access (CFRA) as in LTE, so the overall preambles to be processed during a PRACH occasion could be less than the maximum indicated in Table 2. Also, the quantized $N_{cs}$ values used with restricted sets are different (see [3]) and therefore the maximum radius achievable for different PRACH formats will be different for restricted sets compared to the ones indicated in Table 2. The timing offset estimate error tolerance is related to the SCS configured for the PRACH channel [36]. While selecting the proper PRACH format and $N_{cs}$, the maximum timing offset allowable should be considered. The largest time offset $\Delta \tau$, due to propagation delay cannot be larger than the length of the detection window corresponding to the given $v$ and $N_{cs}$ (see [36]). That is,

$$\Delta \tau < \min \left( \left( T^{RA,\mu}_{CP} - \frac{1}{2} T_{\det} \right), \frac{1}{2} \cdot T_{\det} \right) - \tau_d$$

where $T_{det} = \frac{N_{cs}}{L_{RA}} * 2048 * \kappa * 2^{-\mu} * T_c$. The timing offset ranges for different formats can be then be calculated.

### D. RESOURCE MAPPING FOR PRACH
The time-continuous signal $s^{(p,\mu)}_l (t)$ on antenna port $p$ for PRACH is defined (see [3]) by,

$$s^{(p,\mu)}_l (t) = \sum_{k=0}^{L_{RA}-1} a^{(p,RA)}_k$$
$$\times e^{j2\pi \left( k+Kk_1+\bar{k} \right) \Delta f_{RA} \left( t-N^{RA}_{CP,l} T_c - t^{RA}_{start} \right)} \quad (12)$$

The terms in the above equations are defined in section 5.3.2 of [3]. The PRACH resource mapping parameters of interest are $k_1$ and $\bar{k}$. The factor $K = \frac{\Delta f}{\Delta f_{RA}}$, is required as $k_1$ is defined in multiples of $\Delta f$. In this section we will discuss only
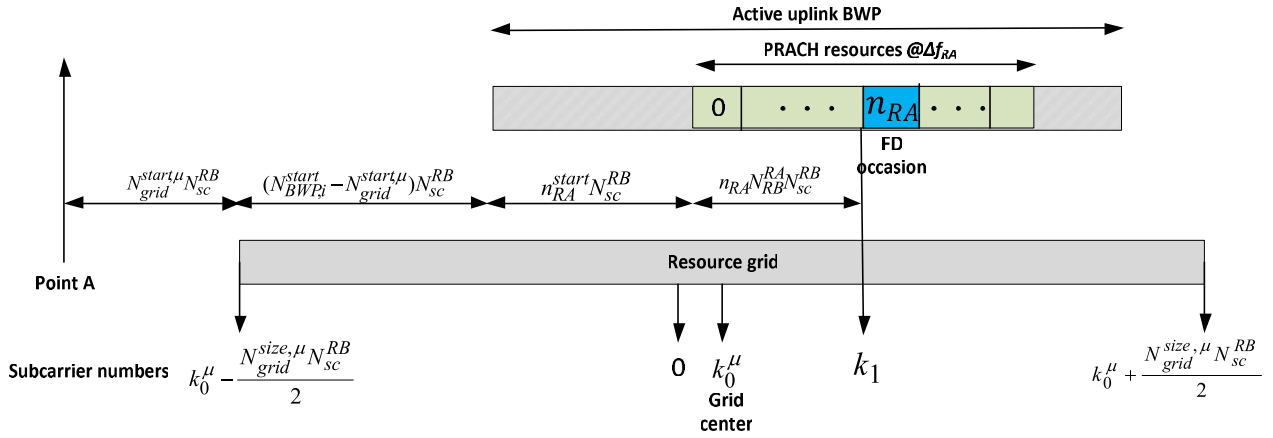
**FIGURE 15.** Location of PRACH transmission occasion within the resource grid.

the relevant terms used in PRACH signal resource mapping, which are required for correct tone extraction at gNB receiver.

### E. DETAILS ON THE SUB-CARRIER OFFSET $k_1$

The term $k_1$ (is in multiples of $\Delta f$) is used to locate the lowest subcarrier of the lowest PRB of the PRACH transmission occasion in frequency domain ($n_{RA}$) with respect to the start of the corresponding resource grid, as illustrated in Figure 15 (also see [15]). $k_1$ is given by (section 5.3.2 of [3]),

$$k_1 = k_o^\mu + (N_{BWP,i}^{start} - N_{grid}^{start,\mu})N_{sc}^{RB} + n_{RA}^{start}N_{sc}^{RB} +$$

$n_{RA}N_{RB}^{RA}N_{sc}^{RB} - \frac{N_{grid}^{size,\mu}N_{sc}^{RB}}{2}$. The parameter $k_0^\mu$ is the sub-carrier offset from the middle subcarrier of numerology $\mu$ to the carrier center frequency $f_0$ and as described in section III-B. Here, the term $k_0^\mu - N_{grid}^{size,\mu}N_{sc}^{RB}/2$ represents the start of the resource grid; the term $n_{RA}^{start}N_{sc}^{RB}$ represents the start of the lowest PRACH transmission as a frequency offset with respect to the start of the active uplink BWP; the term $n_{RA}N_{RB}^{RA}N_{sc}^{RB}$ represents the start of the current (or target) PRACH transmission, and is the frequency offset from the start of the lowest (or first) PRACH transmission; and the term $N_{BWP,i}^{start}N_{sc}^{RB}$ is the frequency offset between Point A and the start of the active uplink bandwidth. Here, $(N_{BWP,i}^{start} - N_{grid}^{start,\mu})N_{sc}^{RB}$ is the frequency offset between resource grid and active uplink bandwidth part. Note that $\Delta f$ is the subcarrier spacing of the initial active uplink bandwidth part during initial access (for CBRA). Otherwise (for CFRA), $\Delta f$ is the subcarrier spacing of the active uplink bandwidth part. Also, $n_{RA}^{start}$ cannot point to PRACH resources outside of the active BW (see [33]).

### F. DETAILS ON THE SUB-CARRIER OFFSET $\bar{k}$

$\bar{k}$ (defined in table 6.3.3.2-1 of [3]) is the subcarrier offset (in multiples of $\Delta f_{RA}$) from PUSCH RB corresponding to the PRACH frequency domain occasion index $n_{RA}$ to the actual random-access subcarrier. This is illustrated in Figure 16 (see [16]) with an example. The details of the below example

(in Figure 16) are as follows, $L_{RA} = 839$ with $\Delta f_{RA} = 1.25$ kHz and $\Delta f = 15$kHz. PRACH bandwidth is then $839 \times \Delta f_{RA} = 1048750\,Hz$. 6 RBs at $\Delta f = 6 \times 12 \times \Delta f = 1.08MHz$. Unused bandwidth is then 31250Hz (or 25 tones @$\Delta f_{RA}$). Note that the PRACH resource offset $\bar{k}$ starts from the middle of the PUSCH subcarrier (i.e., $\frac{\Delta f}{2}$) as in LTE. Therefore, 7.5kHz should be subtracted from 31250Hz on either side, which leaves 13 unused tones @$\Delta f_{RA}$ ( = 16.25kHz). Out of these 7 tones are not used at the start, which is represented by the parameter $\bar{k}$ and 6 tones are not used at the end as shown in Figure 16. PRACH resource referencing is from the mid of the PUSCH sub-carrier (i.e., from $\frac{\Delta f}{2}$) as in LTE (see [20]). Calculations for short preamble (i.e., $L_{RA} = 139$) with $\Delta f_{RA} = 120$kHz and $\Delta f = 120kHz$ (see Table 3 above) are as follows. PRACH bandwidth is $L_{RA} \times \Delta f_{RA} = 139 \times 120 \times 10^3 = 16.68MHz$ In terms of PUSCH RBs (12 RBs from Table 3) this is $N_{RB}^{RA} \times \Delta f \times 12 = 17.28MHz$. Guard tones = 600kHz, which is 5 tones @120kHz. With $\bar{k} = 2$ for this case, 2 zero tones are in the beginning to PRACH start (i.e., with $\bar{k} = 2$ in the Figure 16) and 2 zero tones are at the end of PRACH (with $\frac{\Delta f}{2}$ guard, there will be 2 tones at $\Delta f_{RA} = 120$kHz).

## V. IMPORTANT ASPECTS OF PRACH RECEIVER DESIGN

In this section, all important aspects of PRACH receiver design will be discussed. Specifically, aspects which need to be addressed while designing a PRACH receiver in 5G-NR are presented along with some real system use cases.

### A. PRACH RECEIVER FLOW

A typical non-coherent PRACH receiver processing chain is shown in Figure 17 The data CP is removed from the received time domain signal and $N_{FFT}$ point FFT is taken to obtain the frequency domain (FD) samples. The FD samples are correlated with the configured root sequences. Since the UE's would have used random preamble indices for transmission, several hypotheses, starting from the start root sequence and
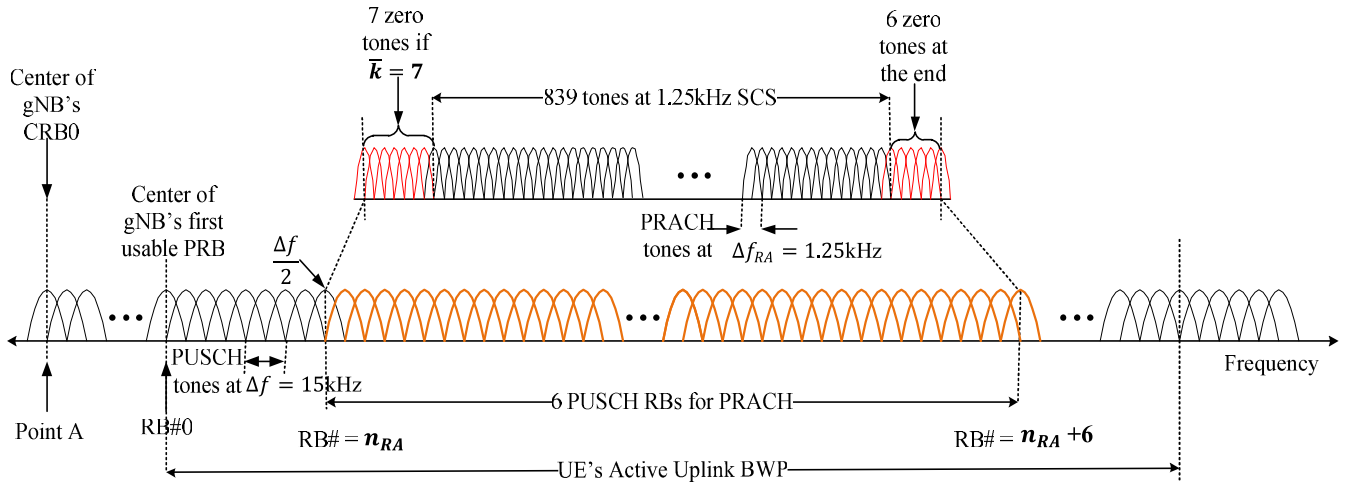
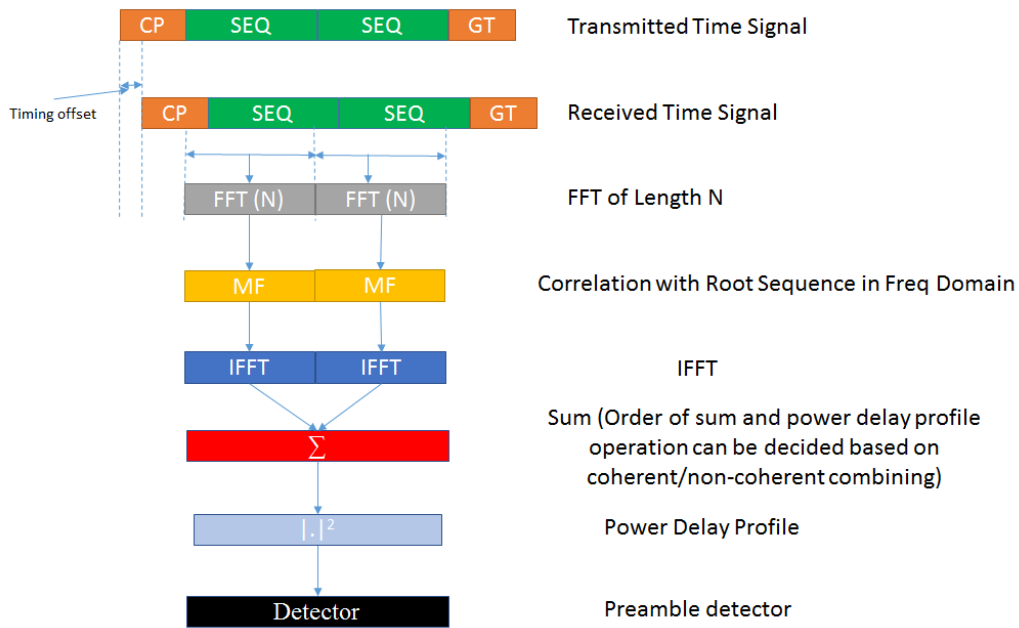**FIGURE 16.** $\bar{k}$ is offset to RA subcarrier from PUSCH subcarrier.



**FIGURE 17.** A typical non-coherent PRACH receiver processing chain [37].

up to number of root sequences configured will be used for detection purposes at gNB. Note that correlation in FD corresponds to complex multiplication of received FD samples with the root sequences. Cross correlation is followed by a time domain energy analysis (using an IFFT) to detect correlation peaks and their exact location within the detection window. With a non-coherent PRACH detector, for each of the received antennas and symbols, the received preamble can be processed independently, and time domain energies can be combined before peak detection. However, the performance and complexity of the non-coherent detector may not be desirable for PRACH formats with higher repetitions which are expected to operate in low SNR regimes. The

complexity here is due to use of an IFFT being used per root/symbol/antenna/TD/FD occasion which could prove to be a bottleneck for most systems. Coherent detection offers lower complexity and better detection gains but will require combining of the received PRACH symbols (and/or antennas) before correlation and time domain analysis. Coherent combining of PRACH symbols will require a few additional processing steps before correlation and time domain analysis can be performed. Specifically, two additional steps will be required before coherently combining the received PRACH symbols. First, the common phase correction which is typically applied in the DFE for data channels, must be undone for PRACH processing. Second, the timing offset introduced due

**TABLE 3.** Subcarrier offset for PRACH resources.

| $L_{RA}$ | $\Delta f_{RA}$ for PRACH in kHz | $\Delta f$ for PUSCH in kHz | $N_{RB}^{RA}$ (allocation expressed in number of PUSCH RBs) | $\bar{k}$ |
|---|---|---|---|---|
| 839 | 1.25 | 15 | 6 | 7 |
| . | …… | …. | … | .. |
| . | …… | …. | … | .. |
| | | | | |
| 139 | 120 | 120 | 12 | 2 |

to data CP removal must be compensated before combining. The details associated with these processing steps are defined in the following sections.

## B. TONE EXTRACTION

The first step though is to extract the required PRACH tones for processing, using all the sub-carrier offsets used in the OFDM signal generation. Consider the case when $\Delta f_{RA} = \Delta f_{data}$ and where a common wideband FFT is used. The first starting tone index for the $n_{RA}^{th}$ frequency occasion is given by (see Figure 16),

$$
N_{toneIndex}^{n_{RA}}
$$
$$
= \overbrace{\frac{\left(N_{FFT} - N_{grid}^{size} N_{SC}^{RB}\right)}{2} - k_0^{mu}}^{\text{Guard tones}}
$$
$$
+ \overbrace{\left(N_{BWP,i}^{start} - N_{grid}^{start,\mu}\right) N_{sc}^{RB} + n_{RA}^{start} N_{sc}^{RB} + n_{RA} N_{RB}^{RA} N_{sc}^{RB}}^{\text{tone offset to } n_{RA} \text{ freq.occasion}}
$$
$$
+ \overbrace{\bar{k}}^{\text{subcarrier offset}}. \tag{13}
$$

Simplifying we get (see derivation of $k_1$ and $\bar{k}$ in section IV-E and IV-F), $N_{toneIndex}^{n_{RA}} = \frac{N_{FFT}}{2} + Kk_1 + \bar{k}$, where $Kk_1$ and $\bar{k}$ are defined in sections IV-E and IV-F and $N_{FFT}$ is the wideband FFT size. Here, the factor $K$ is required because $k_1$ will be in units of $\Delta f$ (see section IV-E). Starting from $N_{toneIndex}^{n_{RA}}$, $L_{RA}$ number of tones can be extracted for PRACH receiver processing.

## C. UNDO COMMON PHASE CORRECTION

During the up-conversion to the carrier frequency $f_{UE}$ (or $f_0^{BWP}$, see section III-B), there is no common phase correction term applied at the UE for PRACH transmission (see section 5.4 of [3]). However, due to the use of common DFE chain between PRACH and data channels, common phase correction which is done for data channels (typically within DFE) should be undone for PRACH processing if a coherent detector is being used. This phase per-symbol for OFDM symbol index $l$ is given by $e^{-i\theta_l}$, where, $i = \sqrt{-1}$, $\theta_l = 2\pi f_0^{gNB}\left(t_{start,l}^{\mu} + T_{CP,l}^{\mu}\right)$, where $f_0^{gNB}$ is the receiver

center frequency of the gNB in Hz. The phase offset for PRACH signal due to the common phase correction should be undone before coherent combining of the PRACH symbols (repetitions). The phase de-rotation term can be computed as follows. Let the PRACH start symbol (column 6 of Table 6.3.3.2-4 in [3]) be denoted as $p_{start} \in \{0, \dots 14\}$ and the number of PRACH repetitions as $N_{rep}^{PRACH} = \frac{N_u}{2048\kappa \cdot 2^{-\mu}}$ (with $N_u$ defined in Table 6.3.3.1-2 of [3]). For the PRACH symbol $p \in \{p_{start} .., p_{start} + N_{rep}^{PRACH} - 1\}$, the accumulated phase is $t_{phase}^{p,s}$ from the reference symbol (i.e., symbol 0 of slot with $\mod\left(n_s^{\mu}, 2^{\mu}\right) == 0$)) to symbol $p$ for slot $s = \mod\left(n_s^{\mu}, 2^{\mu}\right)$. In slot $s$, for the $j$th FFT output and PRACH symbol $p$, the phase de-rotation term will be $e^{i\theta_p} = e^{-2i\pi f_0^{gNB}\left(t_{phase}^{p,s}\right)}$. Since the phase term repeats every 1ms (see derivation in [26]), $t_{start,l}^{\mu}$ will repeat every $2^{\mu}$ or 8 slots. The reference data symbol for phase compensation will be symbol 0 of the slots where phase term repeats, i.e., data symbol 0 of slots with $\mod\left(n_s^{\mu}, 2^{\mu}\right) == 0$. Adding slot notation to $t_{start,l}^{\mu}$ as $t_{start,l}^{\mu,s}$ to denote the accumulated phase in slot $s$, the accumulated phase $t_{phase}^{l,s}$ from the reference symbol to symbol $l$ for slot $s = \mod\left(n_s^{\mu}, 2^{\mu}\right)$, is given by,

$$
t_{phase}^{l,s}
= \begin{cases} t_{start}^{\mu,s-1} + T_c(N_{cp,l=0}^{\mu,s} + (l-1) \times (N_u^{\mu} + N_{cp,l}^{\mu})), & l > 0 \\ t_{start}^{\mu,s-1} + T_c N_{cp,l}^{\mu,s}, & l = 0 \end{cases}
$$
$$\tag{14}$$

with $t_{start,l}^{\mu,s-1} = 0$ for slots with $s = 0$ and $l = 0$. Here, $N_{cp,l}^{\mu}$ is the number of samples in data CP for data symbol $l$ Note that $N_{cp,l=0}^{\mu}$ will be longer by $16\kappa$, for slots $s = 0$ or $2^{\mu-1}$.

## D. TIMING COMPENSATION (DUE TO DATA CP REMOVAL)

One of the design items discussed in 3GPP during the PRACH preamble design in NR was to enable the use of the common wideband FFT (at gNB) for all uplink channels (see [18], [34] and [35]) when the sub-carrier spacing between data and access channels is same as shown in Figure 18. This has a consequence on the PRACH receiver, which may have to account for the data CP removal before the common wideband FFT, especially when a coherent combining of symbols is being considered. The signal within each FFT is a cyclic shifted version of the PRACH preamble sequence and can be easily rotated. However, in case of long formats, a separate DFE chain needs to be present (to cater to 1.25kHz and 5kHz subcarrier spacing) and a common wideband FFT cannot be used. The removal of data CP time samples results in a phase ramp on the frequency domain samples of PRACH and needs to be compensated for in the PRACH receiver if coherent combining across symbols is required. For a PRACH preamble with CP and sequence being repeated several times, each OFDM symbol acts as a cyclic prefix for the next OFDM symbol. However, the OFDM symbols which is repeated has much smaller length as compared to LTE PRACH and equals the same length

as adjacent user data OFDM symbols. The received signal within each FFT window will then act on a cyclic shifted version of the PRACH preamble sequence [18].

With the use of wideband FFT for PRACH, we see that each extracted PRACH symbol consists of two parts of samples coming from adjacent two repetitions (see Figure 18). The timing offset compensation due to this operation needs to be done for proper PRACH detection/timing estimation. The timing offset in the time domain is equivalent to the phase ramping in the frequency domain. After tone extraction, the phase ramping will be implemented for each of the symbols. After tone extraction, denote the frequency domain tone as $X_i^r[k]$, $0 \leq k \leq L_{RA} - 1$, $0 \leq l \leq N$ for each symbol $l$, and each received antenna $r = \{1, \cdots N_{rx}\}$. Here, $N$ is the number of repetitions of a PRACH sequence for a given PRACH format and given by $N = \frac{N_u}{2048\kappa \cdot 2^{-\mu}}$. Denote the phase ramping factor as $\rho_j$ for the $j^{th}$ FFT tick. The phase ramping should start from the tone 0 of 1024 tones since coherent combing will be done subsequently. Since PRACH is not located in the tone 0, the initial phase offset needs to take the initial PRACH tone location into account. The initial phase is $e^{\frac{i2\pi k_2 \rho_j}{N_{FFT}}}$. The phase ramping is $\hat{X}_i^r[n] = X_i^r[n]e^{\frac{i2\pi(n+k_2)\rho_j}{N_{FFT}}}$, where $k_2 = Kk_1 + \bar{k} + \frac{N_{FFT}}{2}$ with $K$, $\bar{k}$ and $k_1$ defined earlier. The phase ramping factor can be computed as,

$$\rho_j = mod\left(\left(N_{CP}^{RA} - N_{CP,l}^{\mu}\right) - (j-1) * N_{CP,l>0}^{\mu}, N_{FFT}\right). \tag{15}$$

Note that for formats Bx, which have guard bands at the end of the PRACH preamble, some of the PRACH symbols will be aligned to left of the PUSCH symbol boundaries and some symbols are aligned to the right of the PUSCH symbol boundaries (see Figure 12). The PRACH symbols which are aligned to the left of the PUSCH symbol will result in $\left(N_{CP}^{RA} - N_{CP,l}^{\mu}\right) - (j-1) * N_{CP,l>0}^{\mu} < 0$ and the phase ramping factor will need to be circularly shifted by $N_{FFT}$ for coherent combining of symbols. Due to the possible frequency offset, it might not be possible to coherently combine all the repetitions without degrading performance. Let $\xi$ is the residual frequency offset between receiver and transmitter, i.e., residual frequency offset is the remaining frequency offset after the downlink synchronization has happened at the UE. In [23], for FR2, $\xi = 4000Hz$ was assumed during simulations and the phase rotation over 1 PRACH symbol will be $2\pi \times \xi \times \left(T_s \times \left(N_u^{\mu}\right)\right) = 6°$. This angular rotation seems small enough to combined adjacent symbols.

### E. TIMING OFFSET ESTIMATION
The IFFT size ($\geq L_{RA}$) determines the timing offset resolution of the PRACH receiver. There will be $\left\lfloor\frac{N_{ifft}}{L_{RA}}\right\rfloor$ samples in time domain to analyse for a peak per root. The number of windows to analyse will be $\left\lfloor\frac{N_{ifft}}{N_{CS}}\right\rfloor$. For $\Delta f_{RA} = 120kHz$ and $L_{RA} = 139$, the timing resolution with $N_{ifft} = 144$ will be $\frac{1}{120kHz}{144} \approx 57.87ns$. This has to converted to some multiple of

minimum resolution of timing advancement, therefore the peak detection index should be appropriately quantized. From section 4.2 of [7], the initial time alignment value $N_{TA} = T_A \cdot 16 \times 64 \times T_c/2^{\mu}$, with index values of $T_A = 0, 1, 2, \ldots, 3846$. The lowest resolution (with $T_A = 1$) for $\mu = 3$ is then $1 \times 16 \times \frac{64}{8} \times \left(\frac{1}{480*1e3*4096}\right) \approx 65ns$, which is basically $\frac{0.52\mu s}{2^{\mu}}$ in terms of LTE resolution. Note that the detection metric must be normalized with noise and compared with a threshold for a correct detection. The detection threshold for each format and $N_{cs}$ can be determined by using the method described in [42]. Noise estimation can be based on unused roots or cyclic shifts. It can also be made based on the IFFT energy. In all estimations however, the estimated noise variance has a signal energy component bias, which seems to be the negligible while using unused roots. For all the parameters discussed so far, an example use case is as follows. For a mmW system with BW of 100MHz and sub-carrier spacing of 120kHz for both PRACH and data channels, the common wide-band FFT size would be $\frac{f_s}{\Delta f_{data}} = \frac{122.88Msps}{120kHz} = 1024$. The IFFT size for PRACH detection and timing analysis could be $N_{ifft} = 192$ leading to a timing estimate resolution of $\approx 43.4ns$. The timing estimate windows can be split into positive and negative windows (in some proportion) around a given centre sample to be able to detect positive and negative timing offsets respectively, depending on gNB requirements.

## VI. PRACH RECEIVER IMPLEMENTATION ASPECTS
### A. PROCESSING COMPLEXITY
The IFFT module used for time domain analysis in the PRACH receiver often dictates the receiver complexity. This is because, IFFT is typically implemented in hardware and while processing multiple symbols (combined or not) per antenna, per hypothesis (i.e., a given root), per TD/FD occasion with a single IFFT engine could be prove limiting. One can indeed limit the number of roots supported as a gNB capability. Note that some formats may require roots greater than what can be supported by gNB to derive 64 preambles (or whatever is configured by gNB) to obtain maximum coverage offered by the format. In those scenarios, gNB will simply support up to max roots possible by gNB and $N_{cs}$ should be configured appropriately (based on reduced coverage) so that 64 preambles (or the number of preambles to use as configured by gNB) can be derived with the number root sequences which can supported.

Coherent combining provides a better implementation complexity with performance gains as the number of roots to be processed is lower. However, there could be a limit on symbols which can be coherently combined without degrading performance as noted previously (due to frequency offset). Combining across the antennas before detection could also be considered but will require precoding coefficients information associated with the antennas. If precoding information is not available, coherent combining across antennas can be done in time domain after IFFT (as shown in Figure 17).
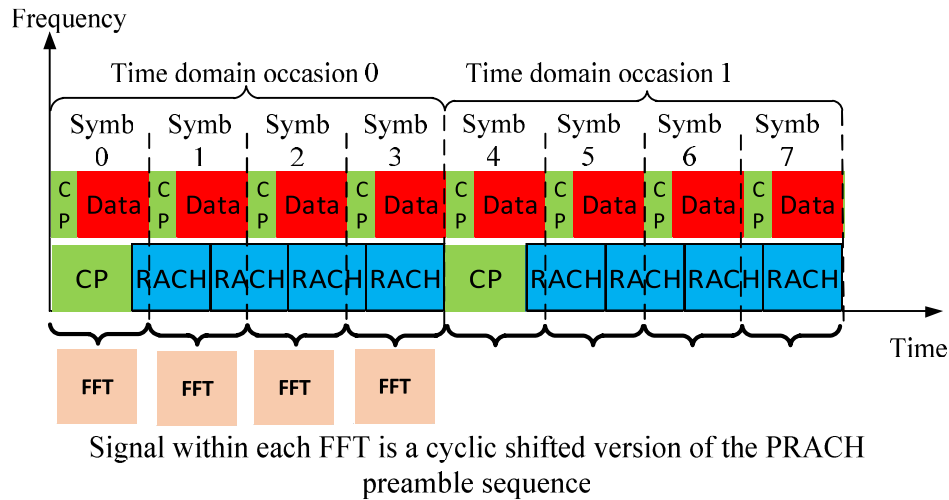
**FIGURE 18.** Common wideband FFT for PRACH with A1 short format and Data.

## B. WIDEBAND FFT USAGE

A note on the wideband FFT usage when $\Delta f_{DATA} \neq \Delta f_{RA}$. For a given bandwidth and sampling rate, FFT size is computed as $N_{FFT} = \frac{f_s}{\Delta f}$, which for 100MHz bandwidth is 1024 for 120kHz SCS, 2048 for 60kHz SCS and so on. When $\Delta f_{DATA} \neq \Delta f_{RA}$ and a narrowband chain is not available, FFT size can be computed based on $\Delta f = \min(\Delta f_{DATA}, \Delta f_{RA})$ so that FFT grid is aligned to the smaller sub-carrier spacing (see Figure 5 in section II-B for different tone alignments). However, when $\Delta f_{DATA} \neq \Delta f_{RA}$, CP removal before wideband FFT would introduce performance degradation on data or PRACH. One way to mitigate the performance loss could be as follows. While using a common FFT with resolution based on lower SCS, FFT window is from end of CP of higher SCS (longer CP) to end of symbol duration of lower SCS. For example, consider $f_s = 30.72Msps$ for a 20MHz BW with $\Delta f_{RA} = 15$kHz and $\Delta f_{DATA} = 30$kHz. Assume, PRACH and data are multiplexed in frequency. Then the normal CP size (in microseconds) of higher SCS is $\frac{4.7\mu s}{2} = 2.35\mu s$ and symbol duration = 33.33 $\mu s$. For lower SCS, CP and symbol sizes are $4.7\mu s$ and $66.66\mu s$ respectively. The FFT size required if only PRACH was present is $\frac{30.72Msps}{15kHz} = 2048$. FFT size if only data was present is $\frac{30.72Msps}{30kHz} = 1024$. Apply a 2048-point FFT after removing $2.35\mu s$ worth of CP samples on $66.66\mu s$ worth time samples. Basically, the FFT captures 1 symbol of 15kHz and 2 symbols of 30kHz. But with this approach, for PRACH, $2.35\mu s$ of CP portion has also been captured. These time samples (before FFT) may have corruptions based on multi-path fading which may affect some portion of the spectrum (depends on the frequency components of that corruption).

If this multi-path is from a previous PRACH signal, the corruption will likely impact PRACH channel. Further, note that 2.5us worth of PRACH symbol end was cut off, because of beginning the FFT earlier than 4.7us. The FFT window for PRACH is basically mis-aligned. Since most PRACH formats

has multiple repetitions symbols to boost SNR, it may be possible to tolerate such signal corruptions due to common wideband FFT usage. Alternatively, CP size worth $4.7\mu s$ could be dropped before computing the FFT. But, $2.35\mu s$ worth of symbol information of higher SCS (PUSCH) will also be removed, which can significantly degrade uplink throughput performance. This may not be acceptable. Also, with a common FFT approach, processing of PUSCH will incur extra delay of 1 symbol which may not be desirable. This is because we are buffering for at least $2.35\mu s+66.66\mu s$ before firing off the FFT. Whereas, PUSCH 1st symbol was already available by $2.35\mu s+33.33\mu s$ mark. Given the above issues, it might be desirable to have separate DFE chains for PRACH and data.

## C. PRACH PROCESSING WITH DELAYS GREATER THAN SYMBOL DURATION

Delays up to the length of one PRACH OFDM symbols can be detected by frequency domain matched filters as outlined in Figure 19 [37]. However, this receiver structure results in a delay ambiguity when the delay exceeds the length of the PRACH OFDM symbol (i.e., $> N_u$). This can happen, for example, while using C2 format with start symbol 0 in slots with longer CP duration. A modified PRACH preamble detector is then required. An example of a PRACH preamble detector for handling large delays (see [35]) is illustrated in Figure 19. Here, a detector is included which compares the received signal in first and last FFT time windows resulting in a decision if delays are smaller or larger than the length of the PRACH OFDM symbol. This decision can then be combined with a delay estimator as in Figure 5-1 (see [35] and [37]) resulting in a timing estimate with high time resolution and support possible propagation delays larger than one PRACH OFDM symbol. Such a large delay estimator may be required when PRACH format C2 needs to be configured. See [35] and [36] for methods on resolving detection ambiguity.
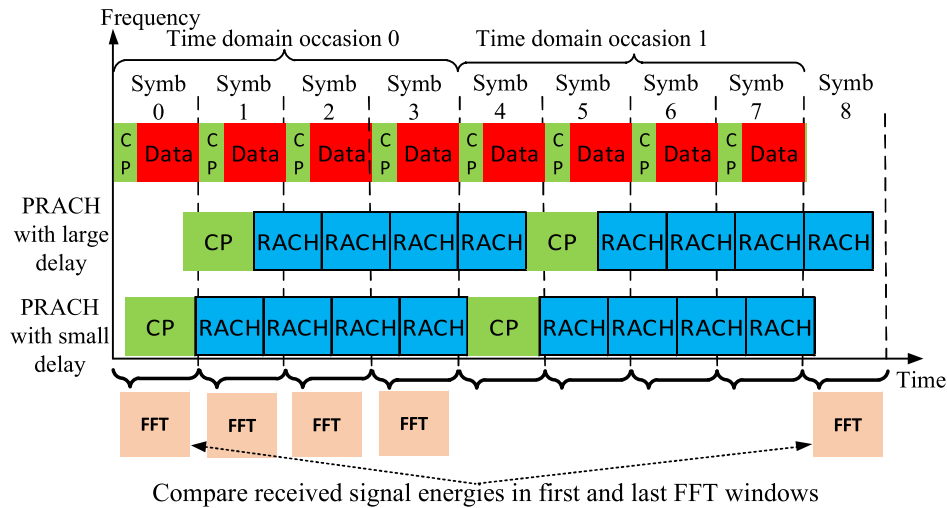
**FIGURE 19.** Small/Large delay PRACH preamble detector outline (see [35]).

**TABLE 4.** RAN4 performance requirements from [6] and [39] and comparison with two different network operators reported performance.

| Results from | Channel (annex J) | $\xi$ in Hz | Min. SNR (dB) for Short Formats in FR2 | | | | | |
|---|---|---|---|---|---|---|---|---|
| | | | A1 | A2 | A3 | B4 | C0 | C2 |
| Table 8.4.1.5.2-2 of [39] | AWGN | 0 | -8.4 | -11.2 | -13.0 | -15.6 | -5.5 | -11.1 |
| Table 11.4.2.2.2-2 of [6] | AWGN | 0 | -8.7 | -11.5 | -13.3 | -15.9 | -5.8 | -11.4 |
| Nokia [40] | AWGN | 0 | -11.43 | -14.45 | -15.78 | -18.48 | -8.43 | -14.42 |
| Ericsson [41] | AWGN | 0 | -11.6 | -14.6 | -16.4 | -19.2 | NA | NA |
| Table 8.4.1.5.2-2 of [39] | TDLA 30-300 Low | 4K | -1.1 | -3.8 | -5.2 | -6.9 | 1.8 | -3.6 |
| Table 11.4.2.2.2-2 of [6] | TDLA 30-300 Low | 4K | -1.7 | -4.4 | -5.8 | -7.5 | 1.2 | -4.2 |
| Nokia [40] | TDLA 30-300 Low | 4K | -4.15 | -7.01 | -8.54 | -11.01 | -1.13 | -7.05 |
| Ericsson [41] | TDLA 30-300 Low | 4K | -4.2 | -7.2 | -8.6 | -9.8 | NA | NA |

## D. RAN4 PERFORMANCE REQUIREMENTS

Radio Performance and Protocol aspect requirements for base station [6] are specified by the 3GPP Radio Access Network working group 4, also known as RAN4 and can be used to bench mark the performance of a PRACH receiver. The performance recommendations made by RAN4 committee for both base-station performance [6] and base-station conformance testing [39] are shown in Table 4 for FR2. The performance recommendations are for AWGN and Tapped

Delay Line (TDL) channel with delay spread of 30 ns and maximum Doppler of 300Hz. The probability of correct detection is defined in section 11.4.2.2.1 of [6] and the minimum requirements are listed in section 11.4.2.2.2 of [6]. PRACH test preambles used for RAN4 performance study are defined in annex A.6 of [6] and delay profiles for each of the channel model is defined in annex G.2.1.1 of [6]. The minimum SNR (in dB) listed in Table 4 is the SNR at which 1% missed detection was achieved, timing error tolerance was less than the values specified in Table 11.4.2.2-1 of [6] and the false alarm was less than 0.1%. Table 4 also lists RAN4 performance reported from Nokia and Ericsson where margins $\geq 3dB$ are seen for most scenarios. A simulation study of the PRACH receiver outlined in this paper, revealed that performance margins were comparable to [40]. Interestingly, these margins could be achieved only with a PRACH receiver using coherent combining of PRACH symbols before detection.

## VII. CONCLUSION

In this paper, downlink and uplink initial access channels in 5G-NR was studied in detail. With the 5G-NR 3GPP specifications details being quite dense getting clear information can prove to be a tedious task. Several design details associated with the physical layer procedures of initial access channels, which are skipped in the 3GPP 5G NR specifications were explained in detail in this paper. Three important contributions were made in paper. First, the design details and justifications associated with both downlink and uplink access channels were discussed. Aspects of signal generation and phase correction were presented with mathematical analysis. Secondly, receiver design aspects of NR PRACH were discussed in detail with illustrating examples. Lastly, implementation aspects of a PRACH receiver and its performance comparisons with 3GPP defined Radio Performance and Protocol aspect requirements or RAN4 requirements were presented for millimeter wave access. The work in this paper will be of

significant value to researchers and system design engineers looking to design efficient initial access algorithms within the framework of 5G-NR systems.

## REFERENCES

[1] MWC. (Mar. 2018). *Small Cells Taking Cellular to New Heights With IoT Tech and Global Deployments.* [Online]. Available: https://www.qualcomm.com/news/onq/2018/03/16/mwc-2018-small-cells-taking-cellular-new-heights-iot-tech-and-global-deployments

[2] J. Liu, K. Au, A. Maaref, J. Luo, H. Baligh, H. Tong, A. Chassaigne, and J. Lorca, "Initial access, mobility, and user-centric multi-beam operation in 5G new radio," *IEEE Commun. Mag.*, vol. 56, no. 3, pp. 35–41, Mar. 2018.

[3] *Technical Specification Group Radio Access Network; Evolved Universal Terrestrial Radio Access; Physical Channels and Modulation*, document TS 36.211 V14.1.0, 3GPP, Dec. 2016.

[4] *Technical Specification Group Radio Access Network; NR; NR and NG-RAN Overall Description, Stage 2*, document TS 38.300 V15.4.0, 3GPP, Jun. 2018.

[5] *General Aspect for UE Radio Frequency (RF) for NR*, document TR 38.817-01 V2.0.0, 3GPP, Jun. 2018.

[6] *Technical Specification Group Radio Access Network; NR; Base Station (BS) Radio Transmission and Reception*, document TS 36.104 V16.2.0, 3GPP, Dec. 2019.

[7] *Technical Specification Group Radio Access Network; NR; Physical Layer Procedures for Control*, document TS 36.213 V15.3.0, 3GPP, Mar. 2018.

[8] *Technical Specification Group Radio Access Network; Evolved Universal Terrestrial Radio Access; and Evolved Universal Terrestrial Radio Access Network, Overall Description*, document TS 36.331 V14.2.0, 3GPP, Mar. 2017.

[9] *Technical Specification Group Radio Access Network; NR; Physical Layer Procedures for Data*, document TS 38.214, V15.3.0, 3GPP, Sep. 2018.

[10] *On DL PTRS Design*, document R1-1705906, 3GPP Contribution, Ericsson, Apr. 2017.

[11] *Summary of 7.1.1.1 Synchronization Signal*, document R1-1807862, 3GPP Contribution, Ericsson, May 2018.

[12] *NR Synchronization Signal Design*, document R1-1708719, 3GPP Contribution, Ericsson, May 2017.

[13] *On k0 for OFDM Signal Generation*, document R1-1805891, 3GPP Contribution, Huawei, May 2018.

[14] *Correcting NR OFDM Symbol Generation*, document R1721601, 3GPP Contribution, Intel, Dec. 2017.

[15] *Remaining Issues on OFDM Baseband Signal Generation*, document R1-1809105, 3GPP Contribution, Sharp, Aug. 2018.

[16] *Ways to Mitigate Frequency Offset With CAZAC Cyclic Shift*, document R1-070227, 3GPP Contribution, LG Electronics, Jan. 2007.

[17] *Limitation of PRACH Sequence Allocation for High Mobility Cell*, document R1-073624, 3GPP Contribution, Panasonic and NTT, Aug. 2007.

[18] *NR PRACH Preamble Design*, document R1-1611904, 3GPP Contribution, Ericsson, Nov. 2016.

[19] *Cyclic-Shift Dimensioning and Capacity Shortfall Solution for Agreed NR PRACH Formats*, document R1-1716686, 3GPP Contribution, Huawei, Sep. 2017.

[20] S. Sesia, I. Toufik, and M. Baker, *LTE, The UMTS Long Term Evolution: From Theory to Practice*. Hoboken, NJ, USA: Wiley, Aug. 2011.

[21] E. Dahlman, S. Parkvall, and J. Skold, *5G NR: The Next Generation Wireless Access Technology*. Amsterdam, The Netherlands: Elsevier, Aug. 2018.

[22] *E-UTRA Random Access Preamble Design*, document R1-060998, 3GPP Contribution., Ericsson, Mar. 2006.

[23] *Simulation Results for PRACH Requirements*, document R4-1815361, 3GPP Contribution, Ericsson, Nov. 2018.

[24] *Remaining Details on PRACH Formats*, document R1-17120277, 3GPP Contribution, Samsung, Dec. 2017.

[25] *Remaining Details on PRACH Formats*, document R1-1802945, 3GPP Contribution, Ericsson, Mar. 2018.

[26] *NR OFDM Symbol Generation Analysis*, document R1-1800296, 3GPP Contribution, Intel, Jan. 2018.

[27] *On Numerology for NR PRACH*, document R1-1711598, 3GPP Contribution, Samsung, Jun. 2017.

[28] *NR BS PRACH Demodulation*, document R4-1812592, 3GPP, Contribution, NTT Docomo, Oct. 2018.

[29] *NR-PRACH Preamble Format Details for Capacity Enhancement and Beam Management*, document R1-1711381 and R1-1712152, 3GPP Contribution, Ericsson and Huawei, Jun./Aug. 2017.

[30] *6.1.1.4.1—Remaining Details on PRACH Preamble Formats for Long/Short Sequence Length*, document R1-1714040, 3GPP Contribution, Ericsson, Aug. 2017.

[31] *On Remaining Details of PRACH Formats and Designs*, document R1-1720624, 3GPP Contribution, InterDigital, Nov. 2017.

[32] *Remaining Details of PRACH Formats*, document R1-1802945 and R1-1800417, 3GPP Contribution, Ericson and Samsung, Mar./Jan. 2018.

[33] *NR-PRACH: Capacity Enhancements and Beam Management*, document R1-1712065, 3GPP Contribution, ZTE, Aug. 2017.

[34] *NR PRACH Preamble Design*, document R1-1611904, 3GPP Contribution, Ericsson, Nov. 2016.

[35] *NR PRACH Design*, document R1-1700298, 3GPP Contribution, Ericsson, Jan. 2017.

[36] *Further Discussions on NR PRACH Requirements*, document R4,1812770, 3GPP Contribution, Ericsson, Oct. 2018.

[37] *PRACH Preamble Design for Capacity Enhancement*, document R1-1711146, 3GPP Contribution, Qualcomm, Jun. 2017.

[38] *NR PRACH Design*, document R1-1702127, 3GPP Contribution, Ericsson, Feb. 2017.

[39] *Technical Specification Group Radio Access Network; NR; Base Station (BS) Conformance Testing Part 2: Radiated Conformance Testing*, document TS 38.141-2, 3GPP, Dec. 2019.

[40] *NR PRACH Design*, document R4-1906366, 3GPP Contribution, Nokia, May 2019.

[41] *NR PRACH Design*, document R4-1815361, 3GPP Contribution, Ericsson, Nov. 2018.

[42] A. Chakrapani, "NB-IoT uplink receiver design and performance study," *IEEE Internet Things J.*, vol. 7, no. 3, pp. 2469–2482, Mar. 2020.

**ARVIND CHAKRAPANI** (Member, IEEE) received the Ph.D. degree in electrical engineering from the University of New South Wales, Sydney, NSW, Australia, in 2011. He is currently a Systems Engineer with Qualcomm Technologies Incorporated (formerly Qualcomm Flarion Technologies), where he is involved in product oriented research in the area of the IoT and 5G NR. His past research interests included resource allocation in LTE MAC schedulers, receiver algorithms for V2V, and NB-IoT. His current research interest includes developing efficient physical layer receiver algorithms for 5G NR.

• • •